Two plant-derived aporphinoid alkaloids exert their antifungal activity by disrupting mitochondrial iron-sulfur cluster biosynthesis

Received for publication, March 15, 2017, and in revised form, August 15, 2017 Published, Papers in Press, August 18, 2017, DOI 10.1074/jbc.M117.781773

Siddharth K. Tripathi[‡], Tao Xu[‡1], Qin Feng[‡], Bharathi Avula[‡], Xiaomin Shi[§2], Xuewen Pan[§3], Melanie M. Mask[¶], Scott R. Baerson[¶], Melissa R. Jacob[‡], Ranga Rao Ravu[‡], Shabana I. Khan[‡‖], Xing-Cong Li[‡‖], Ikhlas A. Khan[‡‖], Alice M. Clark[‡‖], and Ameeta K. Agarwal[‡4]**

*From the [‡]National Center for Natural Products Research, the Divisions of [‖]Pharmacognosy and **Pharmacology, Department of Biomolecular Sciences, School of Pharmacy, University of Mississippi, University, Mississippi 38677, the [§]Verna and Marrs McLean Department of Biochemistry and Molecular Biology, Baylor College of Medicine, Houston, Texas 77030, and the [¶]United States Department of Agriculture, Agricultural Research Service, Natural Products Utilization Research Unit, University, Mississippi 38677*

Edited by F. Peter Guengerich

Eupolauridine and liriodenine are plant-derived aporphinoid alkaloids that exhibit potent inhibitory activity against the opportunistic fungal pathogens *Candida albicans* and *Cryptococcus neoformans*. However, the molecular mechanism of this antifungal activity is unknown. In this study, we show that eupolauridine 9591 (E9591), a synthetic analog of eupolauridine, and liriodenine methiodide (LMT), a methiodide salt of liriodenine, mediate their antifungal activities by disrupting mitochondrial iron-sulfur (Fe-S) cluster synthesis. Several lines of evidence supported this conclusion. First, both E9591 and LMT elicited a transcriptional response indicative of iron imbalance, causing the induction of genes that are required for iron uptake and for the maintenance of cellular iron homeostasis. Second, a genome-wide fitness profile analysis showed that yeast mutants with deletions in iron homeostasis-related genes were hypersensitive to E9591 and LMT. Third, treatment of wild-type yeast cells with E9591 or LMT generated cellular defects that mimicked deficiencies in mitochondrial Fe-S cluster synthesis including an increase in mitochondrial iron levels, a decrease in the activities of Fe-S cluster enzymes, a decrease in respiratory function, and an increase in oxidative stress. Collectively, our results demonstrate that E9591 and LMT perturb mitochondrial Fe-S cluster biosynthesis; thus, these two compounds target a cellular pathway that is distinct from the pathways commonly targeted by clinically used antifungal drugs. Therefore, the identification of this pathway as a target for antifungal compounds has potential applications in the development of new antifungal therapies.

Eupolauridine and liriodenine are plant secondary metabolites that belong to the aporphinoid class of alkaloids that contain a benzylisoquinoline backbone and are widely distributed in a large number of plant families (reviewed in Ref. 1). Eupolauridine has been isolated from Annonaceae and Eupomatiaceae families, whereas liriodenine has been isolated from not only these two families, but also from Magnoliaceae, Menispermaceae, Monimiaceae, and Ranunculaceae families (reviewed in Ref. 2). As with many plant secondary metabolites, both eupolauridine and liriodenine possess a diversity of pharmacological properties. We have previously isolated eupolauridine from the West African tree *Cleistopholis patens* and shown that it exhibits antifungal activity against several human fungal pathogens (3–5). Pan *et al.* (6) have isolated eupolauridine from the Madagascan plant *Ambavia gerrardii* and demonstrated its antiproliferative activity against human ovarian and lung cancer cell lines. Liriodenine has been isolated by our group from *C. patens*, *Liriodendron tulipifera*, and *Guatteria multivenia*, and we have shown that it possesses antibacterial and antifungal activities (5, 7–10). It has also been isolated by several other groups from a variety of plant species, and has been shown to exhibit antibacterial, antifungal, antiviral, antitumor, and antiarrhythmic activities (reviewed in Ref. 11).

The mechanism by which eupolauridine and liriodenine mediate their biological activities has not been studied in great detail. Previous studies on eupolauridine have indicated that it targets DNA topoisomerase II, but the precise mechanism by which it inhibits this enzyme has not been established (4). Inhibition of DNA topoisomerase II has also been reported for liriodenine by some groups; but at least one group has reported that liriodenine does not cause DNA damage in yeast cells (reviewed in Ref. 1). Additional mechanisms proposed for the antiproliferative effects of liriodenine include cell cycle arrest, increased production of the tumor suppressor p53, and induc-

This work was supported, in whole or in part, by National Institutes of Health, Public Health Service, NIAID Grant R01 AI27094 and USDA-ARS Specific Cooperative Agreement number 58-6408-2-0009. The authors declare that they have no conflicts of interest with the contents of this article. The content is solely the responsibility of the authors and does not necessarily represent the official views of the National Institutes of Health.

The transcriptional profiling data described in this article are accessible through the NCBI's Gene Expression Omnibus under accession number GSE101749.

This article contains supplemental Figs. S1–S4 and Tables S1–S7.

[1] Present address: Pathology Dept., Medical School, University of Michigan, Ann Arbor, MI 48109.

[2] Present address: First Affiliated Hospital, Sun Yat-Sen University, No. 58 Zhongshan Er Rd., Guangzhou 510080, China.

[3] Present address: 250 Massachusetts Ave., Novartis Institutes for Biomedical Research, Cambridge, MA 02139.

[4] To whom correspondence should be addressed: National Center for Natural Products Research, School of Pharmacy, University of Mississippi, University, MS 38677. Tel.: 662-915-1218; Fax: 662-915-7062; E-mail: aagarwal@olemiss.edu.

tion of nitric-oxide synthase expression (reviewed in Ref. 11). Thus, the primary mechanisms of action of eupolauridine and liriodenine remain largely unknown. It is interesting to note that both of these compounds may be derived from the same precursor metabolite, liriodendronine, and thus, it is possible that they target the same biological pathways (reviewed in Ref. 12). A detailed characterization of the mechanism of action of this class of compounds will (*a*) facilitate the pharmacological development of these compounds, (*b*) potentially reveal new target pathways for drug development, and (*c*) improve our understanding of how these compounds provide chemical defense to the producing plant species.

In the present study, using the yeast *Saccharomyces cerevisiae* as a model organism, we have conducted genomic, genetic, and biochemical studies to gain insight into the mechanism of action of two compounds that are derivatives of eupolauridine and liriodenine. Eupolauridine 9591 (E9591)[5] is a benzylnapthyridinium analog of eupolauridine, and liriodenine methiodide (LMT) is a methiodide salt of liriodenine. Both compounds exhibit stronger antifungal activities compared with the respective parent compounds. In this work, we show that both E9591 and LMT elicit a transcriptional response indicative of iron depletion, and both compounds show increased activity against mutants lacking genes involved in iron uptake and mitochondrial iron-sulfur (Fe-S) cluster synthesis. Elemental profile analysis revealed that, in contrast to iron chelators that decrease cellular iron levels, E9591 and LMT caused a significant increase in intracellular iron levels. Because an up-regulation of the iron regulon accompanied by an increase in intracellular iron levels is a key feature of yeast cells with deficiencies in mitochondrial Fe-S cluster biogenesis, we further explored if E9591 and LMT disrupted this pathway. We confirmed that E9591 and LMT produced several cellular effects that were consistent with the phenotypes of mitochondrial Fe-S cluster synthesis deletion mutants. Collectively, our results indicate that E9591 and LMT disrupt mitochondrial Fe-S cluster biosynthesis, a pathway not known to be targeted by current antifungal drugs.

Results

Transcriptional responses to E9591 and LMT are indicative of iron depletion

In broth microdilution assays, E9591 and LMT exhibited improved antifungal activities compared with the respective parent compounds. In a previous report, the minimum inhibitory concentration (MIC) of eupolauridine against the fungal pathogens *Candida albicans* and *Cryptococcus neoformans* was reported to be 61.2 and 244.8 μM, respectively (4). In comparison, the MIC of E9591 against these two pathogens was found to be 2.6 and 5.3 μM, respectively (Table 1). This result is consistent with a previous report in which E9591 exhibited a 32-fold improvement in activity against these two pathogens compared with the parent compound (13). Similarly, LMT showed improved activity against *C. albicans* and *C. neoformans* in comparison to the parent compound. In previous reports, the MIC of liriodenine against these two pathogens was found to be 22.5 and 45.4 μM, respectively (8, 10); in contrast, LMT exhibited an MIC of 0.9 and 7.5 μM, respectively (Table 1). This result is in agreement with a previous report in which LMT demonstrated an 8-fold improvement in activity against *C. albicans* compared with the parent compound (8). The activities of E9591 and LMT against *C. albicans* are comparable with the clinically used antifungal drug amphotericin B.

Table 1
Structures of E9591 and LMT and their *in vitro* antifungal activities compared to the antifungal drug amphotericin B (AMB)

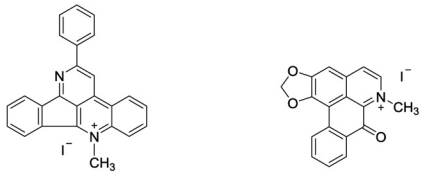

Species[a]	E9591		LMT		AMB	
	IC_{50}[b]	MIC[c]	IC_{50}	MIC	IC_{50}	MIC
C. albicans	0.5[d]	2.6	0.7	0.9	0.6	1.4
C. glabrata	0.6	2.6	16.8	47.9	0.8	1.4
C. krusei	1.4	2.6	1.2	6.0	1.0	2.7
C. neoformans	1.1	5.3	3.6	7.5	0.5	1.4
A. fumigatus	>100	>100	>100	>100	1.3	2.7

[a] Broth microdilution assays were performed according to Clinical and Laboratory Standards Institute guidelines. The media used were RPMI for *A. fumigatus* and *Candida* species, and Sabouraud dextrose for *C. neoformans.* The temperature of incubation was 37°C for *Candida* species, and 30°C for *C. neoformans* and *A. fumigatus.* The strains used were *C. albicans* ATCC 90028, *C. glabrata* ATCC 90030, *C. krusei* ATCC 6258, *C. neoformans* ATCC 90113, and *A. fumigatus* ATCC 90906.
[b] Concentration that results in 50% growth inhibition relative to controls.
[c] MIC, the lowest concentration that allows no detectable growth.
[d] Numbers are in micromolar, and are average values from duplicate experiments.

To understand the mechanism behind the antifungal effects of E9591 and LMT, we conducted transcriptional profiling studies in the model yeast *S. cerevisiae*. Yeast cells were exposed to E9591 and LMT at their respective IC_{50} concentrations for a period of one doubling time (~4 h). Genes exhibiting significant differential expression between compound-treated and solvent-treated cells (p value of $\leq$0.001, fold-change of $\geq$2) were identified. E9591 treatment resulted in the up-regulation of 168 genes, whereas LMT treatment resulted in the up-regulation of 362 genes and the down-regulation of 86 genes (see supplemental Table S1).

The major transcriptional response to E9591 and LMT consisted of the up-regulation of genes that are known to be induced when yeast cells are grown in iron-limiting conditions (Fig. 1*A*, see cluster 1). These genes belong to the iron regulon and are regulated by the transcription factor Aft1 (reviewed in Refs. 14 and 15). Among the Aft1-dependent genes known to be induced under iron deficiency (15–18), E9591 and LMT commonly induced 11 genes. These included genes involved in iron uptake (*ARN1*, *CCC2*, *FIT1*, *FRE2*, *FRE3*, and *FRE5*), iron mobilization from the vacuole (*FET5* and *FTH1*), mitochondrial iron transport (*MRS4*), and genes involved in metabolic adaptation

[5] The abbreviations used are: E9591, eupolauridine 9591; LMT, liriodenine methiodide; Fe-S, iron-sulfur; SD, synthetic dextrose; PHEN, 1,10-phenanthroline; BIPR, 2,2′-bipyridyl; GO, gene ontology; ICP-MS, inductively coupled plasma-mass spectrometry; MIC, minimum inhibitory concentration; BPS, bathophenanthrolinebisulfonic acid.

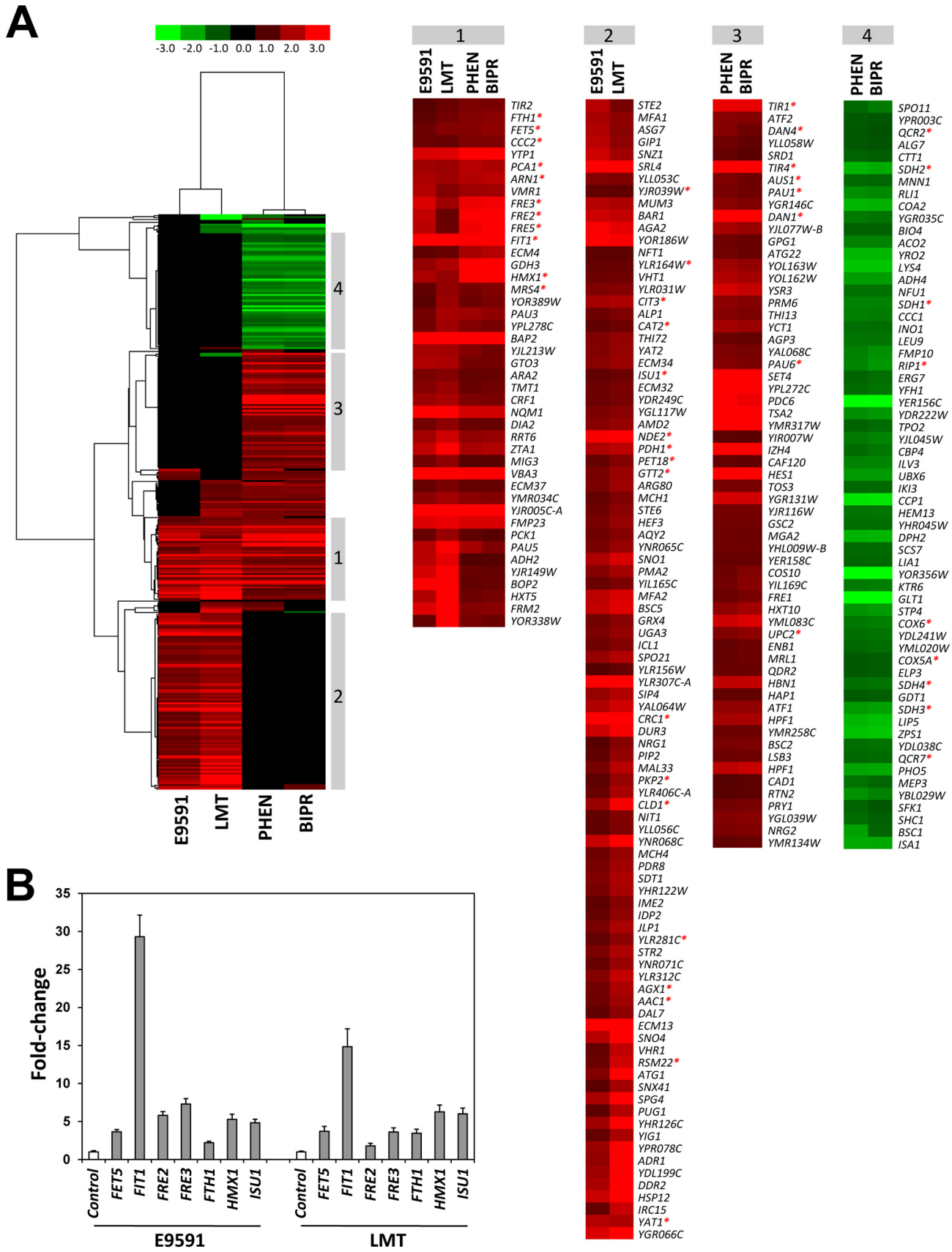
A
-3.0 -2.0 -1.0 0.0 1.0 2.0 3.0
E9591
LMT
PHEN
BIPR
1
2
3
4
TIR2
FTH1*
FET5*
CCC2*
YTP1
PCA1*
ARN1*
VMR1
FRE3*
FRE2*
FRE5*
FIT1*
ECM4
GDH3
HMX1*
MRS4*
YOR389W
PAU3
YPL278C
BAP2
YJL213W
GTO3
ARA2
TMT1
CRF1
NQM1
DIA2
RRT6
ZTA1
MIG3
VBA3
ECM37
YMR034C
YJR005C-A
FMP23
PCK1
PAU5
ADH2
YJR149W
BOP2
HXT5
FRM2
YOR338W
STE2
MFA1
ASG7
GIP1
SNZ1
SRL4
YLL053C
YJR039W*
MUM3
BAR1
AGA2
YOR186W
NFT1
YLR164W*
VHT1
YLR031W
CIT3*
ALP1
CAT2*
THI72
YAT2
ECM34
ISU1*
ECM32
YDR249C
YGL117W
AMD2
NDE2*
PDH1*
PET18*
GTT2*
ARG80
MCH1
STE6
HEF3
AQY2
YNR065C
SNO1
PMA2
YIL165C
MFA2
BSC5
GRX4
UGA3
ICL1
SPO21
YLR156W
YLR307C-A
SIP4
YAL064W
CRC1*
DUR3
NRG1
PIP2
MAL33
PKP2*
YLR406C-A
CLD1*
NIT1
YLL056C
YNR068C
MCH4
PDR8
SDT1
YHR122W
IME2
IDP2
JLP1
YLR281C*
STR2
YNR071C
YLR312C
AGX1*
AAC1*
DAL7
ECM13
SNO4
VHR1
RSM22*
ATG1
SNX41
SPG4
PUG1
YHR126C
YIG1
YPR078C
ADR1
YDL199C
DDR2
HSP12
IRC15
YAT1*
YGR066C
TIR1*
ATF2
DAN4*
YLL058W
SRD1
TIR4*
AUS1*
PAU1*
YGR146C
DAN1*
YJL077W-B
GPG1
ATG22
YOL163W
YOL162W
YSR3
PRM6
THI13
YCT1
AGP3
YAL068C
PAU6*
SET4
YPL272C
PDC6
TSA2
YMR317W
YIR007W
IZH4
CAF120
HES1
TOS3
YGR131W
YJR116W
GSC2
MGA2
YHL009W-B
YER158C
COS10
YIL169C
FRE1
HXT10
YML083C
UPC2*
ENB1
MRL1
QDR2
HBN1
HAP1
ATF1
HPF1
YMR258C
BSC2
LSB3
HPF1
CAD1
RTN2
PRY1
YGL039W
NRG2
YMR134W
SPO11
YPR003C
QCR2*
ALG7
CTT1
SDH2*
MNN1
RLI1
COA2
YGR035C
BIO4
ACO2
YRO2
LYS4
ADH4
NFU1
SDH1*
CCC1
INO1
LEU9
FMP10
RIP1*
ERG7
YFH1
YER156C
YDR222W
TPO2
YJL045W
CBP4
ILV3
UBX6
IKI3
CCP1
HEM13
YHR045W
DPH2
SCS7
LIA1
YOR356W
KTR6
GLT1
STP4
COX6*
YDL241W
YML020W
COX5A*
ELP3
SDH4*
GDT1
SDH3*
LIP5
ZPS1
YDL038C
QCR7*
PHO5
MEP3
YBL029W
SFK1
SHC1
BSC1
ISA1
B
Fold-change
35
30
25
20
15
10
5
0
Control
FET5
FIT1
FRE2
FRE3
FTH1
HMX1
ISU1
E9591
LMT

to low iron (*HMX1* and *VHT1*) (see supplemental Table S1 and Fig. 1*A*, cluster 1). Because these genes are also known to be induced in the presence of iron chelators (19, 20), we also generated transcriptional profiles for the iron chelating compounds 1,10-phenanthroline (PHEN) and 2,2′-bipyridyl (BIPR). The gene expression profiles of all four compounds were highly similar. All four compounds commonly up-regulated 43 genes, the majority of which are involved in maintaining cellular iron homeostasis, further confirming that E9591 and LMT cause an iron depletion response (Fig. 1*A*, see cluster 1).

Interestingly, there were also several notable dissimilarities between the four profiles. For example, 61 genes commonly down-regulated by the iron chelators PHEN and BIPR were not affected by E9591 and LMT (Fig. 1*A*, cluster 4). Many of these genes are involved in cellular respiration and are known to be down-regulated under conditions of iron deficiency (reviewed in Refs. 14 and 15). Similarly, another set of 61 genes commonly up-regulated by the iron chelators PHEN and BIPR were not induced by E9591 and LMT (Fig. 1*A*, cluster 3). Many of these genes are known to be induced under low oxygen conditions and are also affected by cellular heme levels (reviewed in Ref. 21). It is possible that a longer exposure to E9591 and LMT may be required to cause an up-regulation of anaerobic genes and a down-regulation of respiration genes. Finally, a set of 93 genes that were commonly up-regulated by E9591 and LMT were not induced by the iron chelators PHEN and BIPR (see Fig. 1*A*, cluster 2). Many of these genes are involved in mitochondrial functions including mitochondrial Fe-S cluster synthesis (*ISU1*), monocarboxylic acid metabolism (*CAT2*, *CIT3*, *CRC1*, *PDH1*, and *YAT1*), and amino acid metabolism (*AGX1*). Collectively, these results indicate that E9591 and LMT cause additional metabolic changes in yeast cells distinct from those caused by iron chelators. In addition, the chemical structures of both compounds indicate that they lack the functional group(s) required for chelation with iron (see Table 1).

To further validate the transcriptional profiling data, the expression of 7 genes commonly induced by E9591 and LMT representing iron homeostasis-related functions was analyzed by quantitative real-time RT-PCR (Fig. 1*B*). For all seven genes, there was consistent correlation between transcriptional profiling and real-time RT-PCR data, with similar fold-change values observed for the two assays (compare values in Fig. 1*B* with those in supplemental Table S1).

Genome-wide fitness profiles of E9591 and LMT indicate iron homeostasis disruption

To further delineate the molecular pathways targeted by E9591 and LMT, we conducted a genome-wide fitness profile analysis (22, 23) in which we screened a whole-genome collection of pooled haploid yeast deletion mutants against the two compounds. Upon individual validation, we identified 42 haploid deletion mutants that were significantly more sensitive to either E9591 or LMT in comparison with the wild-type strain (see supplemental Table S3). Highly enriched among these were mutants harboring mutations affecting iron ion homeostasis, Fe-S cluster assembly, vesicle-mediated transport, and oxidative stress (Fig. 2*A*). Mutants exhibiting the highest sensitivity to E9591 and LMT included those with mutations affecting high affinity iron uptake (*FET3* and *FTR1*), mitochondrial Fe-S cluster synthesis (*ISU1* and *ISA2*), oxidative stress (*SOD2*), tricarboxylic acid cycle (*ACO1*), and copper uptake (*CTR1*) (see Fig. 2*B*). Four additional mutants with mutations in mitochondrial Fe-S cluster synthesis (*ISA1*, *GRX5*, *SSQ1*, and *CAF17*) were hypersensitive to E9591 or LMT (Fig. 2*A* and supplemental Table S3).

It is worth noting that whereas mutations in genes involved in high affinity iron uptake (*FET3* and *FTR1*) resulted in increased sensitivity to E9591 and LMT, these two genes did not appear to be induced in the 4-h time point transcript profiling results (Fig. 1*A*). One possible explanation for these observations could be the differences in the drug exposure times used in the two experiments (cells used in the fitness profiling analyses were continuously exposed to E9591 or LMT for 2 days; discussed further below).

Of the 42 mutants identified in our study, 12 mutants with mutations in *FET3*, *FTR1*, *CTR1*, *ERG4*, *LEM3*, *RIM8*, *RIM9*, *SNF7*, *UBP3*, *VPS20*, *WHI2*, and *YPK1* were found to be hypersensitive to the iron chelator bathophenanthrolinebisulfonic acid (BPS) in a genome-wide fitness profiling study (19). Mutants with mutations in *FET3*, *FTR1*, and *CTR1* were also found to be hypersensitive to BPS in another genome-wide screen performed with individual deletion mutants (24). These results further suggest that E9591 and LMT disrupt iron homeostasis. However, as was observed in the transcriptional profiles, the fitness profiles of E9591 and LMT were not identical to that of BPS. Several additional mutants that were found to be hypersensitive to BPS in the previous studies were not observed in our study. Thus, it is possible that iron depletion may not be the primary mechanism of action of E9591 and LMT.

E9591 and LMT treatment increases intracellular iron levels

Because the transcript and fitness profiles of E9591 and LMT were indicative of a disruption in iron homeostasis, we investigated whether exposure to the two compounds leads to an alteration in intracellular iron levels in yeast cells. Using the same experimental conditions as employed for transcript profiling, yeast cells were exposed to E9591 and LMT at their respective IC_{50} concentrations and subjected to elemental analysis by inductively coupled plasma-mass spectrometry (ICP-MS). For comparison, cells were also exposed to the iron chelator PHEN. In addition to iron, 7 additional elements (copper,

Figure 1. Gene expression responses to E9591 and LMT, and their comparison to known iron chelators. *A,* hierarchical cluster analysis of 303 genes that displayed a ≥2-fold change (*p* value, ≤0.001) in response to at least two of the four compounds (E9591, LMT, PHEN, and BIPR) were analyzed. Clustering was performed using Gene Cluster 3.0, and the visual presentation of the data were done with Java Tree View. Regions *1*, *2*, *3*, and *4* are expanded on the right to make gene labels legible. Genes highlighted with a *red asterisk* indicate iron homeostasis-related genes in Region 1, mitochondrial function-related genes in Region 2, anaerobiosis-related genes in Region 3, and respiration-related genes in Region 4. The functional categorization of genes clustered within each region is shown in supplemental Table S2. *B,* quantitative real-time RT-PCR analysis for seven iron homeostasis-related genes that responded to E9591 and LMT. Data are shown as mean ± S.D. Control samples were treated with solvent (0.25% DMSO).

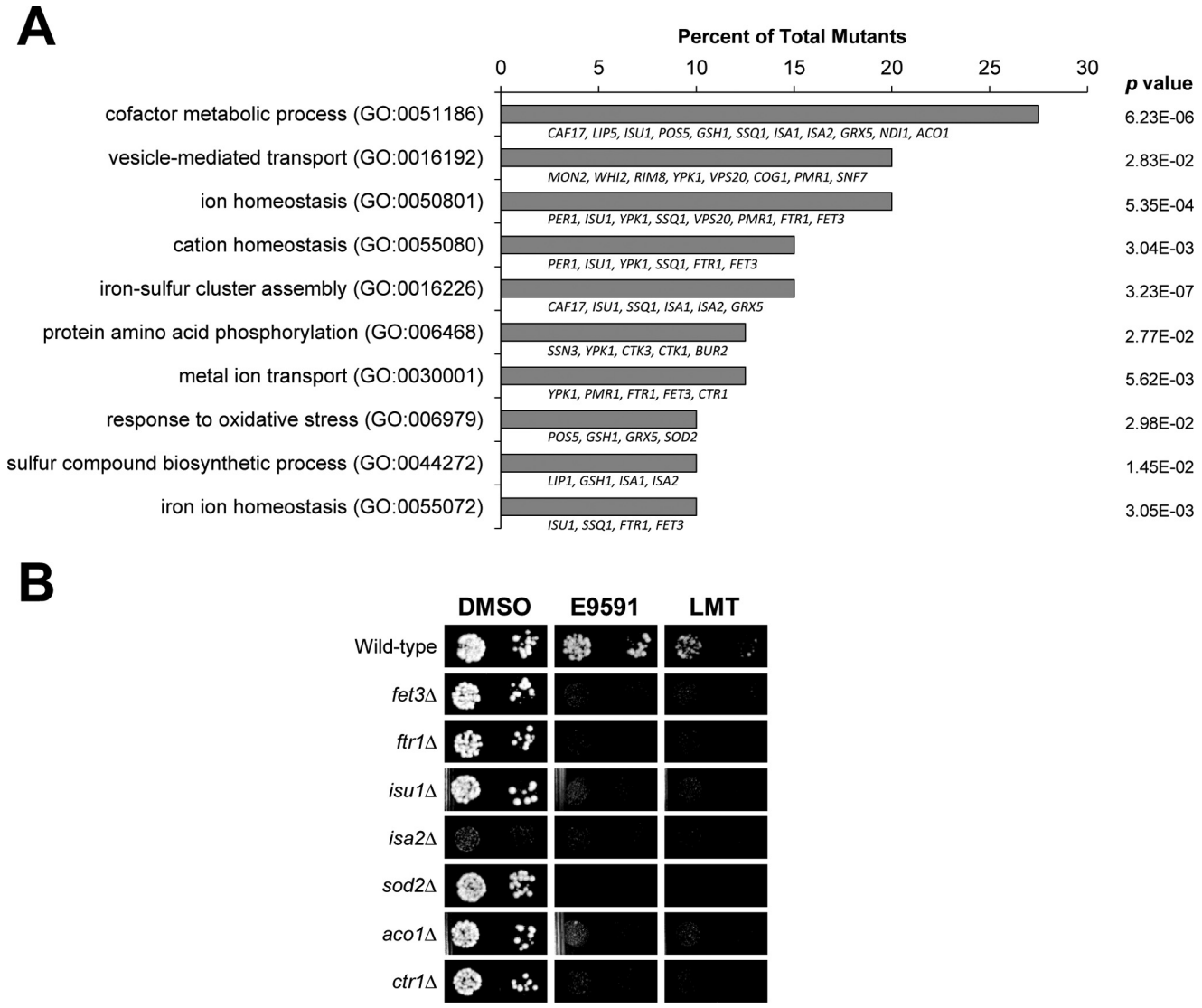

Figure 2. Yeast mutants hypersensitive to E9591 and/or LMT identified by genome-wide fitness profiling analysis. *A*, genes deleted in E9591- or LMT-hypersensitive mutants were distributed into GO categories using the BiNGO tool available in Cytoscape software. The *p* values of significant GO categories are shown on the *right*. Genes present within each GO category are shown *below each bar*. *B,* representative mutants exhibiting the highest level of sensitivity to E9591 and LMT are shown. Haploid-convertible heterozygous diploid deletion mutants of the indicated genotype were spotted on haploid selection medium that either contained or lacked the respective compounds. The *ho*Δ mutant served as a surrogate wild-type control in this study. *DMSO*, medium containing 1% DMSO; *E9591*, medium containing E9591 at 2 μM; *LMT*, medium containing LMT at 1 μM.

manganese, sodium, potassium, magnesium, calcium, and zinc) were quantifiable under these conditions.

As expected, cellular iron levels were decreased (by ~51%) in PHEN-treated cells compared with DMSO-treated cells (Fig. 3*C*). In contrast, an increase in intracellular iron content was observed for E9591-treated (~2-fold) and LMT-treated (~1.6-fold) cells relative to DMSO-treated cells (Fig. 3, *A* and *B*). For copper, manganese, potassium, magnesium, and calcium, no significant changes occurred consistently in response to E9591 and LMT. We observed an increase in copper levels in PHEN-treated cells (Fig. 3*C*), which is consistent with the up-regulation of copper transporters under iron-limiting conditions (reviewed in Ref. 14, 15). An increase in zinc levels and a decrease in sodium levels were observed in cells treated with E9591, LMT, and PHEN, suggesting that these changes were not specific to E9591 and LMT. These results further support the hypothesis that exposure to E9591 and LMT is not associated with a direct depletion of iron from yeast cells and that these two compounds do not function as iron chelators.

The increase in intracellular iron along with an increase in the expression of iron regulon genes is highly reminiscent of the effects observed when yeast cells experience a deficiency in the synthesis of Fe-S clusters (reviewed in Refs. 25–28). Fe-S clusters are cofactors found in proteins that play important functions in respiration, amino acid biosynthesis, DNA repair, and protein translation (reviewed in Refs. 25–28). The assembly of Fe-S clusters requires a complex pathway that first generates Fe-S clusters on scaffold proteins, and then transfers the clusters to acceptor sites within recipient apoproteins (reviewed in Refs. 25–28) (see supplemental Fig. S1 for an overview). Both mitochondrial and cytosolic assembly systems exist in eukaryotic organisms, and the former critically influences iron regulation in yeast (reviewed in Refs. 25–28). Defects in the mito-

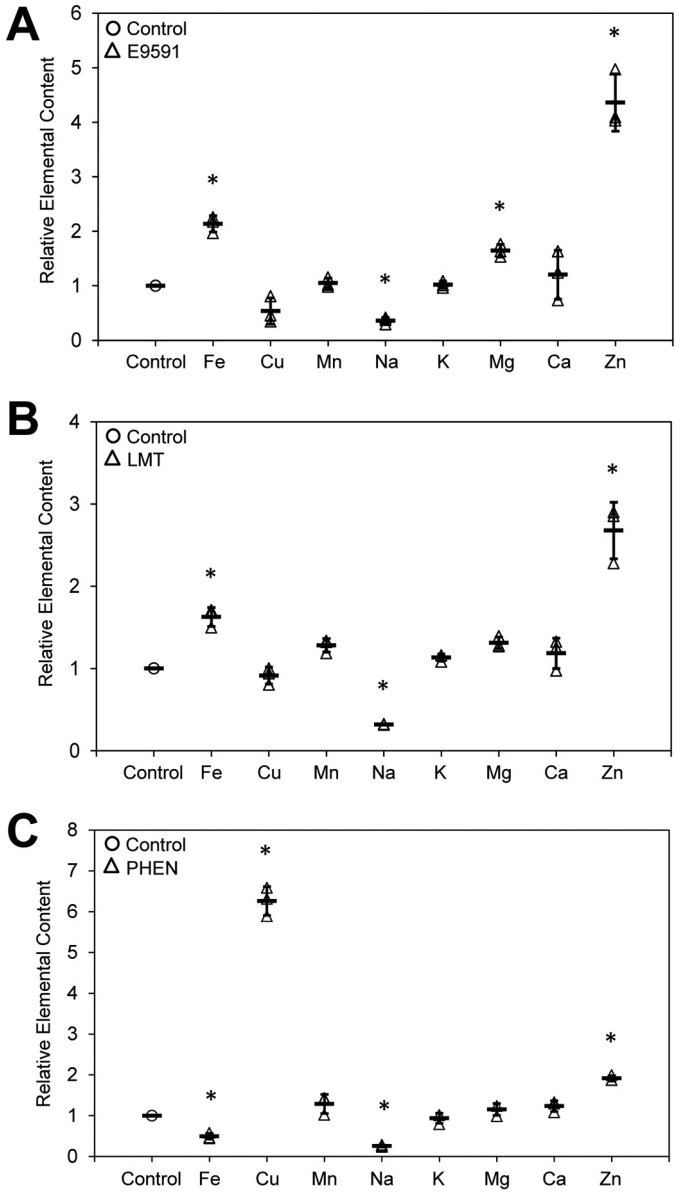

Figure 3. Effect of E9591, LMT, and PHEN on the elemental profile of yeast cells. Yeast cells were grown in the presence of DMSO, E9591, LMT, or PHEN for a period corresponding to ~4.5 doubling times. Total cellular iron content was determined by ICP-MS analysis as described under "Experimental procedures." Values shown are mean ± S.D. from measurements performed on three independent cultures per treatment. Elemental content values are shown relative to the DMSO control values, which were normalized to 1. Statistical significance *versus* DMSO was assessed by an unpaired two-tailed *t* test (*, $p < 0.05$). The absolute elemental content values (in nanograms of element per milligram of yeast cells) for the DMSO control were the following (shown as mean ± S.D.): Fe, 1.7 ± 0.1; Cu, 0.7 ± 0.1; Mn, 1.3 ± 0.1; Na, 83.4 ± 9.6; K, 2244.2 ± 103.9; Mg, 450.1 ± 20.9; Ca, 7.8 ± 0.3; Zn, 7.6 ± 0.2. *A*, effect of E9591 treatment on elemental content. *B*, effect of LMT on elemental content. *C*, effect of PHEN on elemental content.

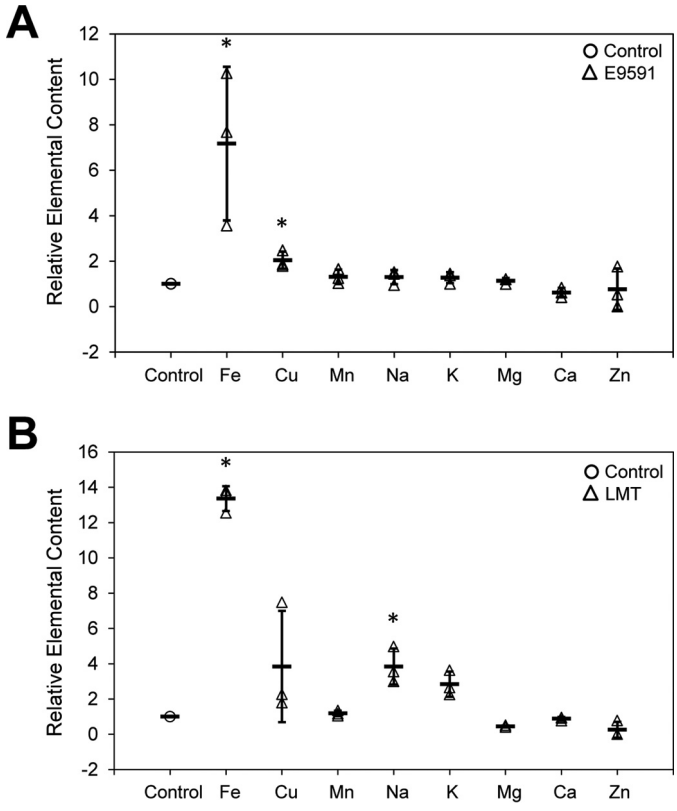

Figure 4. Effect of E9591 and LMT on the elemental profile of yeast mitochondria. Yeast cells were grown in lactate medium in the presence of DMSO, E9591, or LMT for a period corresponding to ~4.5 doubling times. Mitochondria were isolated and iron content was determined by ICP-MS analysis as described under "Experimental procedures." Values are mean ± S.D. from measurements performed on three independent cultures per treatment. Elemental content values are shown relative to the DMSO control values, which were normalized to 1. Statistical significance *versus* DMSO was assessed by an unpaired two-tailed *t* test (*, $p < 0.05$). The absolute elemental content values (in micrograms of element per milligram of protein) for the DMSO control were the following (shown as mean ± S.D.): Fe, 0.4 ± 0.2; Cu, 0.1 ± 0.0; Mn, 0.04 ± 0.0; Na, 71.3 ± 5.6; K, 34.2 ± 1.0; Mg, 4.5 ± 0.5; Ca, 2.3 ± 0.7; Zn, 0.2 ± 0.3. *A*, effect of E9591 on mitochondrial elemental content. *B*, effect of LMT on mitochondrial elemental content.

chondrial Fe-S cluster synthesis pathway results in the disruption of iron homeostasis in yeast cells and an up-regulation of the iron regulon (reviewed in Refs. 14 and 26). This induction results in an increase in iron uptake ultimately leading to an increase in intracellular iron levels (reviewed in Refs. 26 and 28). The excess iron gets distributed to the mitochondria so that the iron demands of this pathway can be met (reviewed in Refs. 25–28). Mitochondrial iron overload has been reported for several mutants in this pathway including those with defects in Isa1, Isa2, Isu1, Isu2, Grx5, Nfs1, Ssq1, Yah1, and Yfh1 (29–37).

To determine whether treatment with E9591 and LMT also caused an overaccumulation of iron in the mitochondria, we monitored mitochondrial elemental levels after exposure to each compound. We observed an approximate 7-fold increase and an approximate 13-fold increase in mitochondrial iron levels in E9591-treated and LMT-treated cells, respectively, compared with DMSO-treated cells (Fig. 4). For the other 7 elements, no dramatic changes were observed to occur commonly in response to E9591 and LMT. It is worth noting that the increase in total and mitochondrial iron levels was observed when yeast cells were exposed to E9591 and LMT for a period of ~15 h (4.5 doublings). This result is consistent with the observed delay in cellular iron accumulation that had been previously noted in Yfh1-depleted cells (38). Taken together, the results shown in Figs. 3 and 4 provide further evidence that the inhibitory effects of E9591 and LMT are likely associated with defects in the mitochondrial Fe-S cluster synthesis pathway.

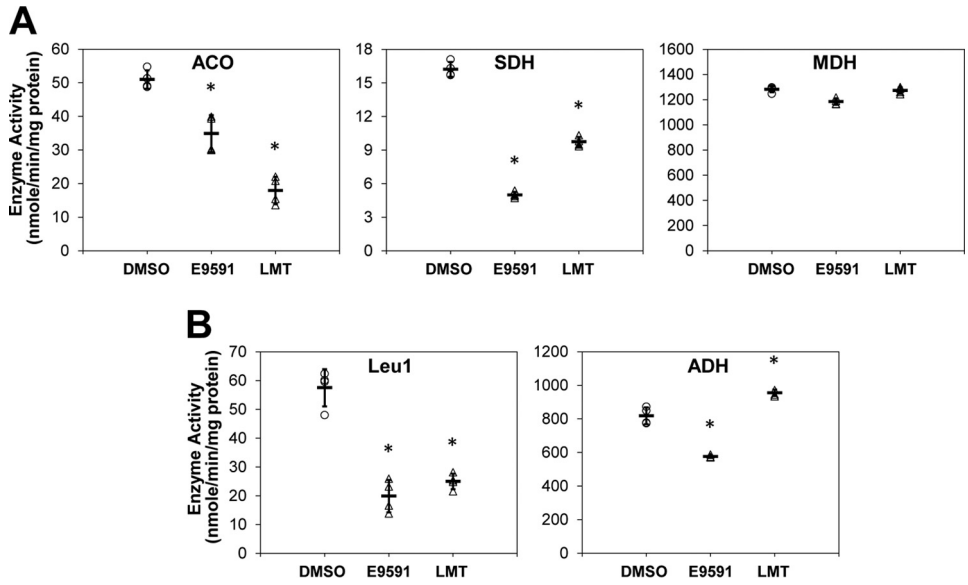

Figure 5. Effect of E9591 and LMT on the activities of mitochondrial and cytosolic Fe-S proteins. *A,* yeast cells (strain S288C) were grown in lactate medium in the presence of DMSO, E9591,or LMT for a period corresponding to ~4.5 doubling times. Mitochondria were isolated, and the enzymatic activities of aconitase (*ACO*), succinate dehydrogenase (*SDH*), and malate dehydrogenase (*MDH*) were determined. Values are mean ± S.D. from a total of four assays performed using two independent cultures per treatment. Statistical significance *versus* DMSO was assessed by an unpaired two-tailed *t* test (*, $p < 0.05$). *B,* yeast cells (strain W303-1A) were grown in Synthetic Complete medium in the presence of DMSO, E9591, or LMT for a period corresponding to ~4.5 doubling times. Cell lysates were prepared, and the enzymatic activities of isopropylmalate isomerase (*Leu1*) and alcohol dehydrogenase (*ADH*) were determined. Values are mean ± S.D. from a total of four assays performed using two independent cultures per treatment. Statistical significance *versus* DMSO was assessed by an unpaired two-tailed *t* test (*, $p < 0.05$).

E9591 and LMT treatment mimics deficiency in mitochondrial Fe-S cluster synthesis

To further confirm that E9591 and LMT have an inhibitory effect on the mitochondrial Fe-S cluster synthesis pathway, we investigated whether treatment with these compounds would mimic additional deficiencies in this pathway. We focused on three phenotypes of mutants in this pathway: a decrease in the activities of the Fe-S cluster-containing enzymes, a deficiency in respiration, and an increase in oxidative stress (reviewed in Refs. 25–28). To maintain consistency with the elemental profile analysis, these experiments were conducted with yeast cells that were exposed to E9591 and LMT for ~15 h (4.5 doublings).

First, we investigated whether treatment with E9591 and LMT affected the enzyme activities of mitochondrial and cytosolic Fe-S proteins. The mitochondrial Fe-S enzymes aconitase and succinate dehydrogenase, and the cytosolic Fe-S enzyme isopropylmalate isomerase (Leu1) have been extensively studied to monitor the effects of deficiencies in the Fe-S cluster synthesis pathway. Decreases in the activities of all three enzymes have been reported in yeast mutants with defects in several Fe-S cluster synthesis proteins including Isd11, Nfs1, Yah1, and Grx5 (32, 33, 36, 39, 40). We observed that when yeast cells were treated with E9591 and LMT, aconitase activity was diminished by 35 and 64%, respectively (Fig. 5*A*). Similarly, treatment of yeast cells with E9591 and LMT caused a reduction in succinate dehydrogenase activity by 70 and 40%, respectively (Fig. 5*A*). In contrast, the activity of mitochondrial malate dehydrogenase as a non-Fe-S control enzyme was not affected (Fig. 5*A*). We also observed that the activity of the cytosolic Fe-S protein Leu1 was decreased by 65 and 56%, respectively, in cells treated with E9591 and LMT, whereas the activity of the control enzyme alcohol dehydrogenase was not strongly influenced by the two compounds (Fig. 5*B*).

Second, we determined if cells treated with E9591 and LMT showed a deficiency in respiration. Respiratory failure is a common trait of mutants deficient in the mitochondrial Fe-S cluster synthesis pathway due to the fact that several Fe-S proteins participate in the respiratory chain. A decline in respiratory function has been observed in mutants with defects in Yfh1, Isu1, Isa1, and Isa2 (29, 31, 37, 38). To determine whether E9591 and LMT treatment causes respiratory deficiency in yeast cells, we monitored the formation of petite (respiration-deficient) mutants upon exposure to these two compounds. This assay is based on the principle that when yeast cells are grown on medium containing glycerol (a non-fermentable carbon source), they are dependent upon mitochondrial respiration, and when grown on medium containing glucose (fermentable carbon source), they can survive without it (reviewed in Ref. 41). We exposed yeast cells to E9591 and LMT, and grew them on media containing glycerol *versus* glucose to determine the number of respiration-competent cells. We observed an approximate 75% reduction in the percentage of respiration-competent cells in E9591-treated and LMT-treated cells compared with DMSO-treated cells (Fig. 6*A*). Petite (small-size) colonies were also clearly visible on the glucose-containing plates for cells treated with E9591 and LMT (Fig. 6*B*). In contrast, when yeast cells were exposed to the iron chelator PHEN under similar experimental conditions, there was no reduction observed in the number of respiration competent cells (see supplemental Fig. S2). Thus, even though the transcriptional responses to E9591 and LMT are indicative of iron depletion, the cellular effects of E9591 and LMT are not reflective of a general impairment in iron metabolism.

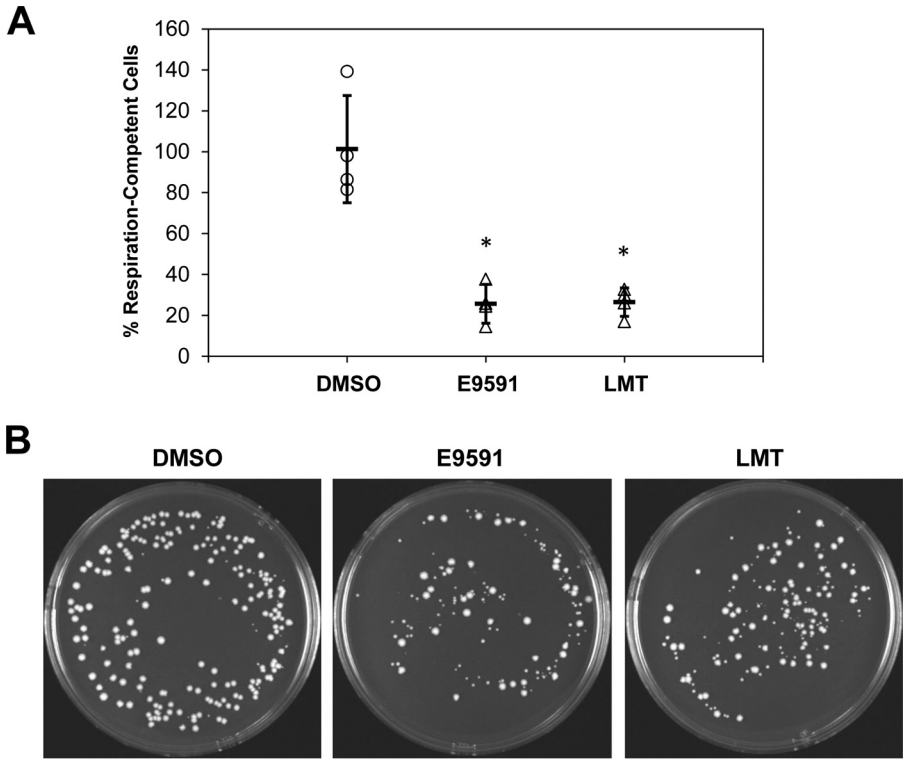

Figure 6. Induction of petite mutant formation by E9591 and LMT. *A,* yeast cells were grown in the presence of DMSO, E9591, or LMT for a period corresponding to ~4.5 doubling times. Samples from each culture were diluted and plated onto YPD (glucose-containing) and YPG (glycerol-containing) plates, and allowed to grow at 30 °C for 3 (YPD plates) to 6 days (YPG plates). The % respiration-competent cells were calculated as follows: number of colonies on YPG/number of colonies on YPD × 100. Data shown are mean ± S.D. from a total of four platings performed using two independent cultures per treatment. Statistical significance *versus* DMSO was assessed by an unpaired two-tailed *t* test (*, $p < 0.05$). *B*, a representative image is shown of a YPD agar plate from each treatment to demonstrate the increased number of small-size colonies in the presence of E9591 and LMT.

Finally, we determined whether E9591 and LMT induced oxidative stress in yeast cells. Oxidative stress is known to be induced in yeast mutants with defects in the mitochondrial Fe-S cluster synthesis proteins Yfh1 and Grx5 (36, 38). This induction is most likely due to the overaccumulation of iron in the mitochondria, which can promote Fenton-mediated formation of reactive oxygen species. To determine whether E9591 and LMT induced oxidative stress in yeast cells, we monitored protein carbonylation levels after exposure to the two compounds. Oxidative stress results in the formation of carbonyl groups on proteins that can be immunodetected by Western analysis. As can be seen in Fig. 7*A*, E9591-treated and LMT-treated cells contained increased levels of carbonylated proteins compared with DMSO-treated cells. We also made use of yeast mutants with deletions in genes required for oxidative stress responses, which exhibit hypersensitivity to chemicals promoting oxidative stress. Mutants with deletions in *YAP1* (encodes a transcription factor required for oxidative stress tolerance), *SOD2* (encodes superoxide dismutase), and *GSH1* (encodes the first enzyme in glutathione biosynthesis) showed increased sensitivity to E9591 and LMT (Fig. 7*B*). It is worth noting that the *sod2*Δ mutant was also identified to be hypersensitive to both compounds in our genome-wide fitness profile analysis (see Fig. 2*B*). We also observed that the iron chelator PHEN did not cause an increase in the levels of carbonylated proteins and the three mutants tested above were not strongly hypersensitive to PHEN (see supplemental Fig. S3). This further suggests that the cellular effects of E9591 and LMT are not due to a general depletion of cellular iron, but rather due to redistribution of iron to the mitochondria. Taken together, the results shown in Figs. 5–7 show that exposure to E9591 and LMT produces effects that are similar to those observed in yeast mutants with defects in the mitochondrial Fe-S cluster synthesis pathway.

Haploinsufficient mutants of mitochondrial Fe-S cluster synthesis genes are hypersensitive to E9591 and LMT

Our genome-wide fitness profile analysis revealed 6 haploid mutants with deletions in the mitochondrial Fe-S cluster synthesis pathway that showed increased sensitivity to E9591 and LMT (see supplemental Table S3). To explore additional mutants in this pathway, we analyzed haploinsufficient mutants that carried heterozygous deletions in 10 different genes required for the biosynthesis and maturation of Fe-S cluster proteins. Because many of the components of the mitochondrial Fe-S cluster synthesis pathway are essential for the viability of yeast cells, mutants containing haploid deletions in them are inviable. Thus, heterozygous deletion mutants allowed us to investigate multiple components of the pathway. As can be seen in Fig. 8, all of the mutants tested showed a strong increase in sensitivity to E9591 compared with the wild-type strain. A clearly discernable increase in sensitivity to LMT was also observed in all mutants, except for the mutant with a heterozygous deletion in *ISA2*, which appeared to show reduced sensitivity to LMT. The reason for this mutant's lack of sensitivity to LMT is unclear at this time. For comparison, we also analyzed

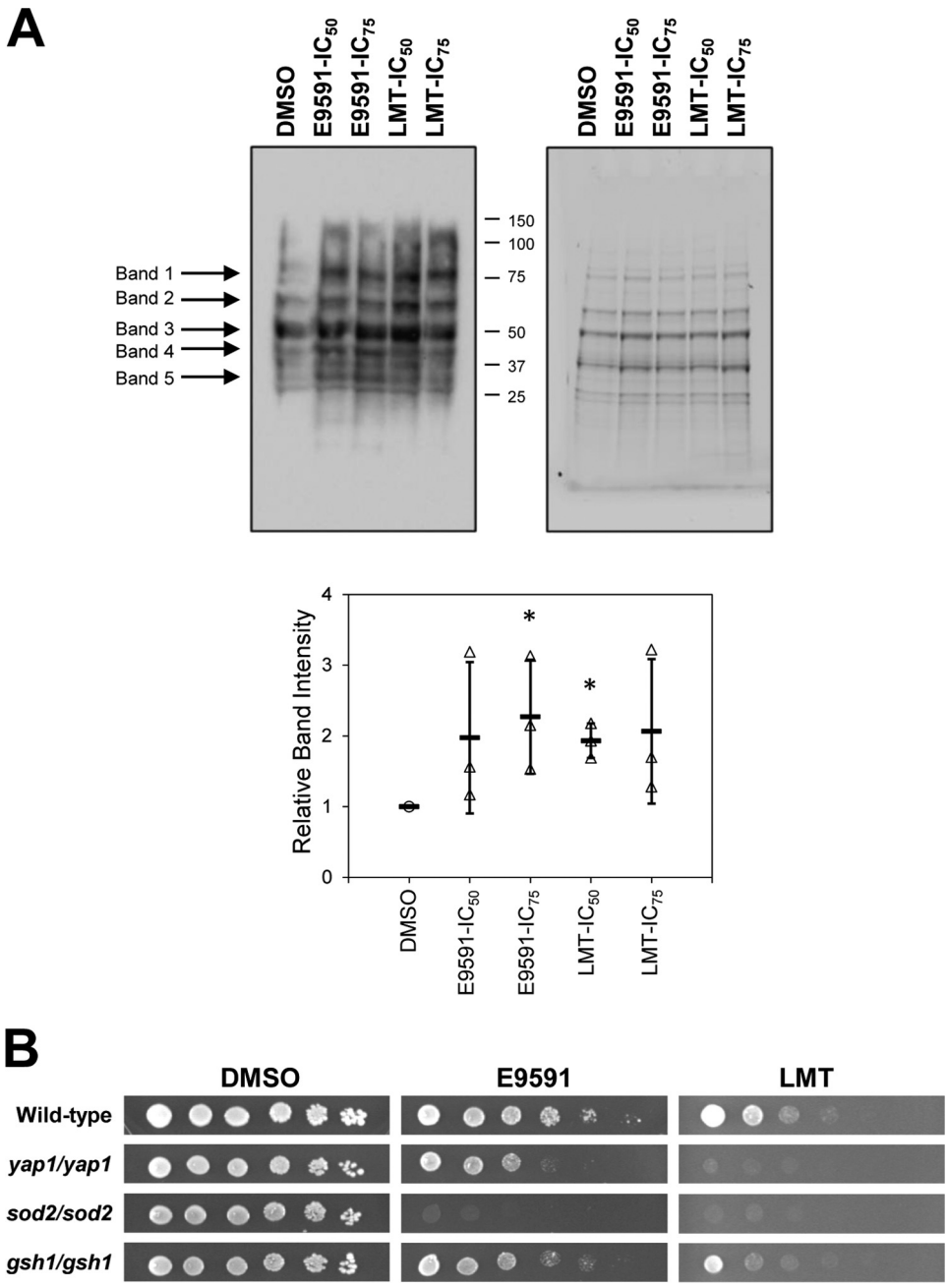

Figure 7. Oxidative stress-related effects of E9591 and LMT. *A*, yeast cells were grown in the presence of DMSO, E9591, or LMT for a period corresponding to ~4.5 doubling times. Carbonylated proteins were detected by Western blot analysis using anti-2,4-dinitrophenol antibodies. Three experiments were performed in total, and the image shown is from one representative experiment. The *right panel* shows a stained protein gel on which aliquots of the same samples were separated. Band intensities for the five most prominent bands (marked with *arrows*) were quantitated with Bio-Rad's Image Lab software, using the total protein normalization tool. The combined total values from all 5 bands were obtained for each treatment and normalized to the DMSO control values. Values shown in the graph are mean ± S.D. Statistical significance *versus* DMSO was assessed by an unpaired two-tailed *t* test (*, $p \leq 0.05$). *B*, the wild-type strain (BY4743) and mutant strains harboring homozygous deletions in 3 different oxidative stress-related genes were grown overnight in YPD-7 (YPD medium, MOPS buffered, pH 7.0) broth. Dilutions (5-fold) were prepared from each culture, inoculated on YPD-7 agar, and incubated for 3 days at 30 °C. *DMSO*, medium containing 1% DMSO; *E9591*, medium containing E9591 at 4 μM; *LMT*, medium containing LMT at 5 μM.

these 10 mutants for sensitivity to the iron chelator PHEN, and the mutants did not exhibit strong hypersensitivity to PHEN (see supplemental Fig. S4). These results further indicate that E9591 and LMT likely cause perturbations within the mitochondrial Fe-S cluster synthesis pathway.

It is worth noting that although three of the 10 genes tested above are not essential genes (*ISA1*, *ISA2*, and *NFU1*), deletions in them resulted in increased sensitivity to E9591 and LMT (with the exception of *ISA2*, which only affects sensitivity to E9591). Interestingly, although there is a tendency for haploinsufficient genes to be essential, there are indeed several examples in the literature where both essential and non-essential genes exhibit haploinsufficiency (*e.g.* Refs. 42–44). It has been suggested that essential genes may represent direct targets of a drug, whereas non-essential genes may exhibit synthetic interactions with the drug targets or the target pathways. In fact,

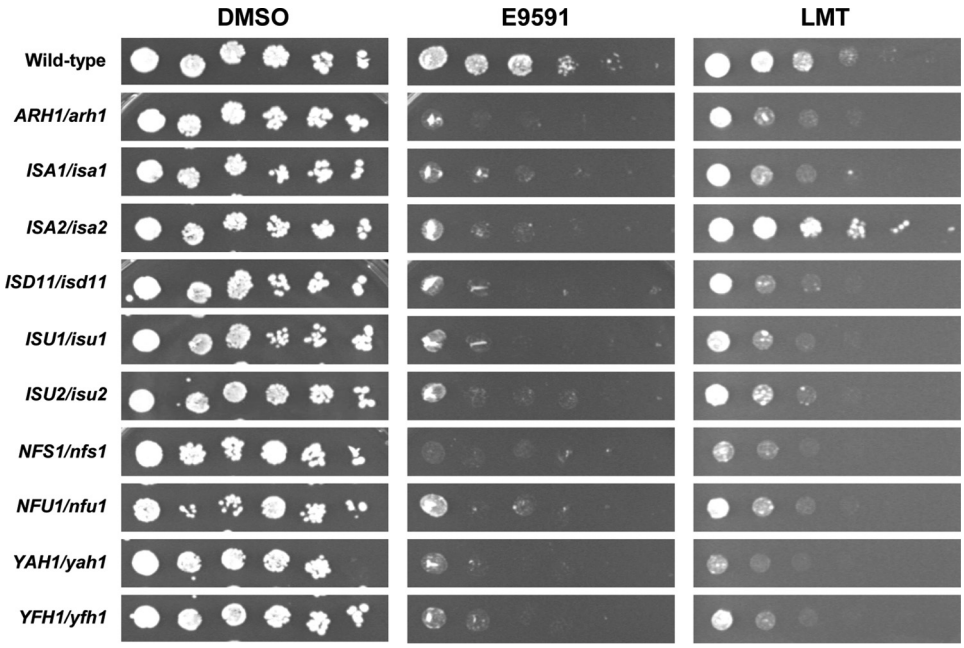

Figure 8. Effect of E9591 and LMT on haploinsufficient mutants of Fe-S cluster synthesis genes. The wild-type strain (BY4743) and mutant strains harboring heterozygous deletions in 10 different Fe-S cluster synthesis genes were grown overnight in YPD-7 (YPD medium, MOPS buffered, pH 7.0) broth. Dilutions (5-fold) were prepared from each culture, inoculated on YPD-7 agar, and incubated for 4 days at 30 °C. *DMSO*, medium containing 1% DMSO; *E9591*, medium containing E9591 at 4 μM; *LMT*, medium containing LMT at 5 μM.

ISA1, *ISA2*, and *NFU1* show physical and genetic interactions with genes involved in the mitochondrial Fe-S cluster synthesis pathway. For example, Isa1 physically interacts with Nfu1 (45). In addition, *ISA2* genetically interacts with *GRX5* (36), and *NFU1* genetically interacts with *ISU1* and *SSQ1* (37). Based on this as well as the results shown in Figs. 4–7, it is highly likely that the increased sensitivity of these three mutants to E9591 and/or LMT is associated with a disruption in mitochondrial Fe-S cluster synthesis caused by the two compounds.

Long-term exposure to E9591 and LMT reveals prolonged effects of mitochondrial Fe-S cluster synthesis disruption

Because the results shown in Figs. 3–7 were observed after yeast cells were exposed to E9591 and LMT for ~15 h, we were also interested in determining the long-term effects of E9591 and LMT. We, therefore, conducted a transcript profiling study on yeast cells that were exposed to E9591 and LMT for ~15 h grown under the same culture conditions as described above. A total of 956 genes were commonly up-regulated and 652 genes were commonly down-regulated by both E9591 and LMT (see supplemental Table S4). The responding genes were organized into GO-based functional categories and overrepresented GO categories were identified (see supplemental Table S5 and Fig. 9).

In agreement with the observed long-term effects of E9591 and LMT on Fe-S cluster enzymes (see Fig. 5), 15-h exposures to E9591 and LMT resulted in the induction of iron regulon genes (see supplemental Table S4). Interestingly, the high affinity iron transporter genes *FTR1* and *FET3*, which were not induced at the 4-h time point, were significantly induced ($p \leq 0.001$) at the 15-h time point. *FTR1* was induced 8.5-fold by E9591 and 3.9-fold by LMT at the 15-h time point (see supplemental Table S4). *FET3*, although not as strongly affected as *FTR1*, was induced 1.9-fold by E9591 and 1.5-fold by LMT at the 15-h time point (see supplemental Table S6, which shows significant iron regulon genes induced by ≥1.5-fold; $p \leq 0.001$). Thus, under the experimental conditions we have employed, a longer exposure to E9591 and LMT, which would likely result in the prolonged disruption of iron homeostasis, may be necessary to elicit the induction of the high affinity iron transporter genes *FTR1* and *FET3*.

Although several iron regulon genes were induced by E9591 and LMT at the 15-h time point, the major overrepresented functional categories among the up-regulated genes included translation, ribosome biogenesis, rRNA processing, amino acid metabolism, nucleotide metabolism, and sterol metabolism (Fig. 9*A*). The up-regulation of genes involved in amino acid and ergosterol metabolism has been previously observed in mutants defective in Yah1 and Atm1 (46), and their induction may occur due to the requirement for several heme-containing enzymes or Fe-S cluster-containing enzymes in these two processes (reviewed in Refs. 15 and 28). Similarly, an up-regulation in nucleotide metabolism genes has been reported in a mutant defective in Grx5 (47), and could be attributed to the requirement for the iron-containing enzyme ribonucleotide reductase in nucleotide biosynthesis (reviewed in Ref. 48). In addition, a large number of genes that participate in protein translation were induced upon long-term exposure to E9591 and LMT (Fig. 9*A*). This induction could occur due to the fact that several proteins required for protein translation contain Fe-S clusters in their structures including Rli1, Elp3, and Twy1 (reviewed in Ref. 28).

As expected, "respiration" was the major functional category for genes down-regulated in response to long-term exposure to E9591 and LMT (Fig. 9*B*). A large number of genes encoding

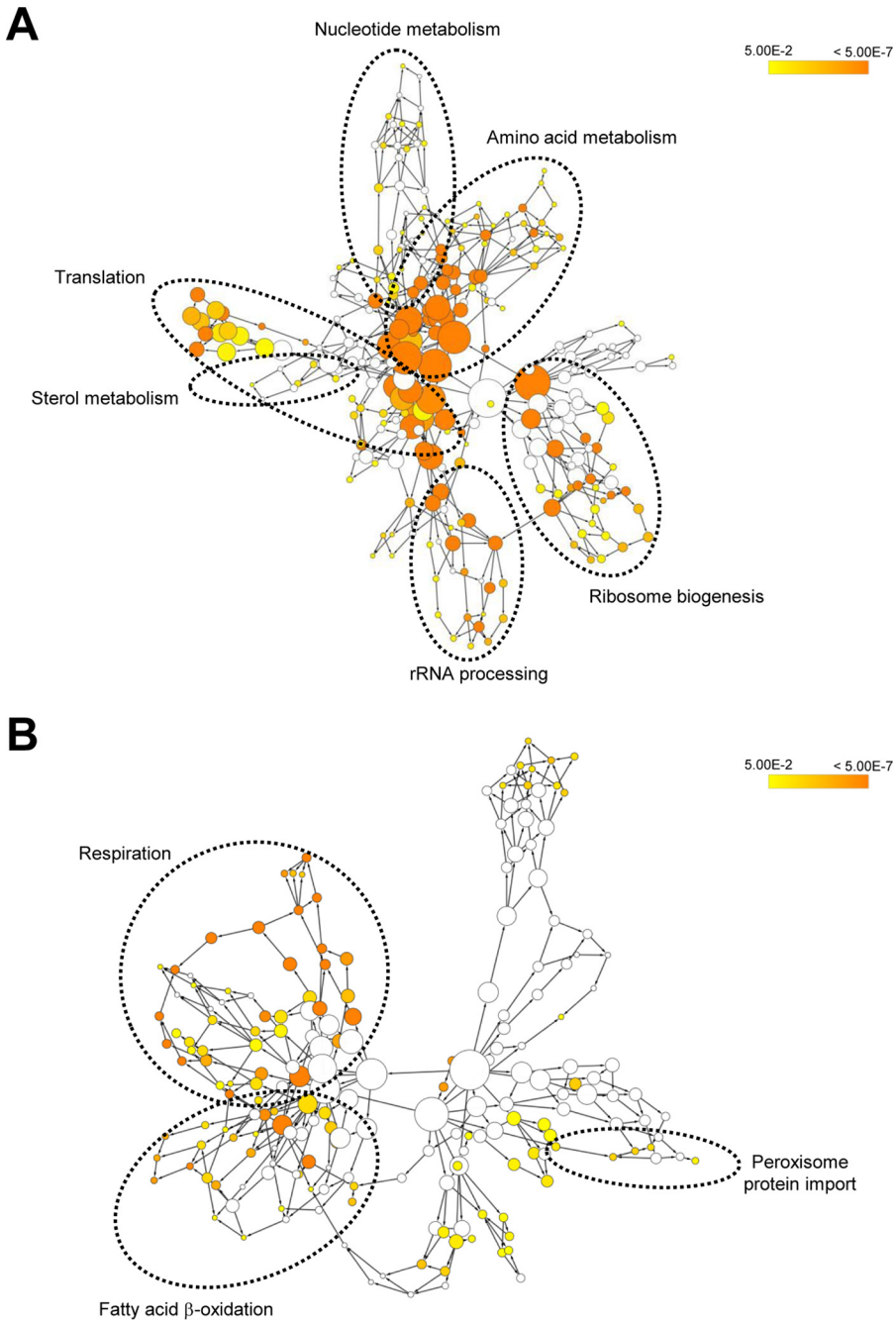

Figure 9. GO-enrichment analysis of genes responding to long-term exposure to E9591 and LMT. 956 up-regulated genes and 652 down-regulated genes commonly responding to E9591 and LMT upon long-term exposure were organized into GO-based biological process categories using the BiNGO plug-in in Cytoscape software. GO categories of interest are highlighted in *black circles*. *A,* GO-enrichment analysis of up-regulated genes. *B,* GO-enrichment analysis of down-regulated genes. The Cytoscape data are provided in supplemental Table S5.

components of the mitochondrial respiratory chain and the TCA cycle are known to be down-regulated in yeast mutants with defects in Yah1, Atm1, and Grx5 (46, 47). Unexpectedly, we also observed that long-term exposure to E9591 and LMT resulted in the down-regulation of genes involved in peroxisome protein import and fatty acid β-oxidation, an important peroxisomal process in yeast cells (Fig. 9*B*). Down-regulation of peroxisomal genes has not been previously observed in mutants with defects in the mitochondrial Fe-S cluster synthesis pathway, and could be attributed to differences in culture conditions between our study and previous studies. The implications of this down-regulation are discussed below.

In summary, the majority of gene expression changes due to long-term effects of E9591 and LMT are similar to those observed in mutants defective in Fe-S cluster synthesis. They are also consistent with the known involvement of Fe-S cluster proteins in diverse biochemical pathways including heme biosynthesis, amino acid and nucleotide metabolism, and DNA repair. It is important to note that the possibility cannot be discounted at present that in addition to affecting the activities

of Fe-S enzymes, E9591 and LMT may also affect the activities of non-Fe-S enzymes that use iron as a co-factor including heme-containing proteins (*e.g.* cytochrome complexes) as well as non-heme iron proteins (*e.g.* ribonucleotide reductase).

Discussion

Using a combination of genomic, genetic, and biochemical approaches, we have shown that the antifungal activity of the plant-derived aporphinoid alkaloids E9591 and LMT is likely mediated by a disruption in the mitochondrial Fe-S cluster synthesis pathway. This conclusion is based on several lines of evidence from the present work: (i) the transcriptome response to E9591 and LMT showed an induction in iron regulon genes, (ii) a genome-wide fitness profile analysis showed that yeast mutants with deletions in iron homeostasis-related genes were hypersensitive to E9591 and LMT, (iii) treatment with E9591 and LMT caused cellular defects that mimicked deficiencies in mitochondrial Fe-S cluster synthesis including an increase in mitochondrial iron levels, a decrease in the activities of Fe-S cluster enzymes, an increase in respiratory deficiency, and an increase in oxidative stress, and (iv) haploinsufficient mutants with deletions in 10 different genes involved in mitochondrial Fe-S cluster synthesis showed increased sensitivity to E9591 and LMT. Thus, these two compounds target a cellular pathway that is distinct from the pathways targeted by current clinically used antifungal drug classes, which are known to work by interacting with membrane ergosterol (*e.g.* polyenes), disrupting ergosterol biosynthesis (*e.g.* azoles), and inhibiting the synthesis of cell wall glucans (*e.g.* echinocandins) (reviewed in Ref. 49).

Because Fe-S proteins play important roles in many different cellular processes including respiration, TCA cycle, amino acid biosynthesis, DNA synthesis and repair, and protein translation, a defect in the synthesis of Fe-S proteins has a severe impact on diverse cellular functions (reviewed in Refs. 25, 26, and 28). In addition, most of the components of the mitochondrial Fe-S cluster synthesis pathway are essential for the viability of yeast cells (reviewed in Refs. 25, 26, and 28). Thus, this pathway could serve as a highly effective target for inhibiting fungal growth. However, due to the importance of Fe-S clusters in all eukaryotes, a therapeutic drug that targets Fe-S cluster synthesis could most likely lack specificity for the fungal pathogen. Nevertheless, specificity could be achieved due to differences between fungal and mammalian proteins that are components of this pathway. For example, the transfer of Fe-S clusters from the Isu1 scaffold protein to target apoproteins requires a dedicated Hsp70 chaperone. Mammalian cells make use of the multifunctional Hsp70 of the mitochondrial matrix, whereas yeast cells utilize a specialized Hsp70 chaperone, Ssq1 (reviewed in Ref. 26). Unlike multifunctional Hsp70s that bind to a large variety of hydrophobic substrates, Ssq1 selectively recognizes and interacts with a conserved peptide loop in Isu1 (50). Also, in yeast cells an additional scaffold protein, Isu2, is used for Fe-S cluster synthesis that is not present in mammalian cells (reviewed in Refs. 26 and 28). Yeast cells with a deletion in either Ssq1 or Isu2 exhibit respiratory deficiency, an increase in mitochondrial iron, and a loss of mitochondrial aconitase activity (30, 37). Thus, Ssq1 and Isu2 have the potential to serve as fungal-specific targets for new antifungal therapies.

By demonstrating that E9591 and LMT function as disruptors of the mitochondrial Fe-S cluster synthesis pathway, this work has identified a promising new pharmacological tool for the further characterization of this pathway in eukaryotic organisms. Given that many of the genes encoding components of this pathway are essential genes, previous studies have made use of conditional mutants that require the mutant cells to be grown under restrictive conditions that impose additional stress on the cells. A chemical inhibitor of this pathway will facilitate these studies and will prevent the occurrence of secondary metabolic effects exerted by restrictive growth conditions. In addition, chemical inhibitors will be of great value in improving our understanding of why defects in mitochondrial Fe-S cluster synthesis result in various human diseases. Human diseases such as Friedreich's ataxia (Yfh1 deficiency), microcytic anemia (Grx5 deficiency), cerebellar ataxia (Atm1), and others are associated with defects in this pathway, and the direct functional connection to this pathway remains to be determined for some of these diseases (reviewed in Refs. 25, 26, and 51). Elucidating the physiological consequences of Fe-S cluster synthesis defects will provide a better understanding of how these diseases occur.

Of further interest, the present work also indicates that disruption of the mitochondrial Fe-S cluster synthesis pathway causes a down-regulation of peroxisomal genes. Previous studies have indicated that perturbations in mitochondrial functions such as those caused by petite mutations cause an up-regulation of peroxisomal genes (52). It was suggested that to compensate for the absence of a complete TCA cycle, respiratory-deficient cells reconfigure their metabolism by activating peroxisomal activities. This ensures that metabolites such as acetyl-CoA that are generated by the β-oxidation of fatty acids in the peroxisomes are made available to the TCA cycle. However, an interruption in mitochondrial Fe-S cluster synthesis causes not only respiratory deficiency but also an overaccumulation of intracellular iron. Given that citrate is known to enhance iron toxicity, one way to control this toxicity would be to reduce intracellular citrate levels. This is supported by the fact that the iron toxicity in a Yfh1-deficient mutant is attenuated by a deletion in the *CIT2* gene, which encodes a peroxisomal citrate synthase (53). It is, therefore, possible that a shutdown in peroxisomal functions could cause a reduction in intracellular citrate levels, allowing the cells to cope with the excess iron that accumulates in Fe-S cluster synthesis mutants. Thus, it is conceivable that under conditions of Fe-S cluster synthesis deficiency, coping with iron toxicity takes precedence over providing metabolites to the TCA cycle. Further studies will be required to understand the molecular mechanisms potentially involved in the cross-talk between mitochondrial Fe-S cluster synthesis and peroxisomal function.

It is worth noting that, although increased intracellular zinc levels were observed following a 15-h exposure to E9591 and LMT (see Fig. 3), increased expression of the zinc transporter genes *ZRT1* and *ZRT2* was not observed. Instead, we observed a down-regulation of *ZRT2* and also a down-regulation of *ZAP1*, *ZRG7*, *ZRG8*, and *ZRG17* (see supplemental Table S4), all of which are required for maintaining zinc homeostasis in yeast cells (*e.g.* Refs. 54 and 55). The transcription factor Zap1

and its target genes are activated under zinc-deficient conditions in yeast cells, and inactivated under zinc excess conditions (reviewed in Refs. 14 and 56). Thus, it is possible that the excess zinc accumulating during the 15-h exposure to E9591 and LMT led to the down-regulation of zinc homeostasis genes. Additionally, it is possible that zinc transporters are only transiently induced, then subsequently down-regulated once intracellular zinc levels increase. A more detailed time course study will be required to examine the possible temporal effects of E9591 and LMT on zinc transporter expression.

Although yeast cells appear to respond to the overaccumulation of zinc, it is not likely that the excess zinc contributes to the phenotypic effects generated by E9591 and LMT. First, long-term exposure of yeast cells to excess zinc has been shown to cause a decrease in intracellular iron content (57). In contrast, E9591 and LMT increased intracellular iron levels. Second, a genome-wide mutant analysis in the presence of excess zinc primarily identified genes involved in vacuolar function (57), and did not identify any iron uptake genes or Fe-S cluster synthesis genes, many of which were identified in the fitness profile of E9591 and LMT. Interestingly, zinc suppresses the phenotypes of a yeast mutant deficient in the Fe-S cluster synthesis protein Yfh1 (58). Excess zinc in the medium prevented mitochondrial iron accumulation in the mutant, and also increased its growth rate as well as resistance to oxidative stress (58). Thus, it is possible that zinc overaccumulation in response to E9591 and LMT may be associated with a mechanism that allows the cells to cope with disruptions in the Fe-S cluster synthesis pathway.

This study lays the groundwork for future studies to determine the precise mechanism of action of E9591 and LMT. Although our data strongly suggest that these compounds disrupt the mitochondrial Fe-S cluster synthesis pathway, further analysis will be required to determine the precise step(s) in the pathway they inhibit and the mechanism or mechanisms involved in this inhibition.

Experimental procedures

Yeast strains, media, and chemicals

S. cerevisiae strain S288C was used for all experiments. Haploinsufficient mutants lacking Fe-S cluster synthesis genes were obtained from Open Biosystems (Huntsville, AL). Synthetic dextrose (SD) medium consisted of 2% (w/v) dextrose and 0.7% (w/v) yeast nitrogen base without amino acids. The medium was buffered with 0.2 M MOPS and the pH was adjusted to 7.0. YPD medium consisted of 1% (w/v) yeast extract, 2% (w/v) peptone, 2% (w/v) dextrose. Lactate medium for mitochondria isolation was prepared as described by Amutha *et al.* (59). For the genome-wide fitness profiling test, the haploid selection synthetic medium was prepared as described previously (22). Dimethyl sulfoxide (DMSO), PHEN, and BIPR were obtained from Sigma. LMT and E9591 were synthesized as described previously (8, 13). The purity of the two compounds was greater than 95% based on TLC and NMR analysis.

Transcriptional profiles of E9591, LMT, PHEN, and BIPR

S. cerevisiae strain S288C was used in the transcriptional profiling experiments, and all procedures including IC_{50} determinations were performed as previously described (60). For the transcriptional profiling study, an overnight culture of *S. cerevisiae* S288C was used to inoculate 50 ml of SD medium to an A_{600} of 0.1. Three replicate cultures were started for each treatment. After one doubling, each culture was treated with E9591, LMT, PHEN, or BIPR at a concentration equivalent to the IC_{50} value (0.053, 2.6, 6.2, and 65.9 μM, respectively). Control cultures were simultaneously treated with 0.25% (v/v) DMSO. The cultures were allowed to grow until an A_{600} of 0.5 was reached (~4 h). For long-term exposure experiments, all experimental conditions were the same except cells were exposed to drug treatments for 4.5 doublings (~15 h). Cells were harvested by centrifugation, flash frozen in liquid nitrogen, and stored at −80 °C.

RNA isolation, target preparation, and hybridizations were performed as described previously (60). The Affymetrix GeneChip Yeast Genome 2.0 array was used in all experiments. Image analysis, scaling, and probe-set-level data analysis was performed using the Affymetrix GeneChip Operating Software. Differentially expressed genes were identified using BRB Array Tools software (61), and genes with $p \leq 0.001$ were considered to be significant. Gene annotations were obtained from the *Saccharomyces* Genome Database. Hierarchical cluster analysis was performed with Gene Cluster 3.0 (62), and the data were visualized with Java Tree View (63). The BiNGO plug-in in Cytoscape software was used for Gene Ontology (GO) analysis, and over-represented GO terms ($p < 0.05$) were identified (64). The transcriptional profiling data described in this article are accessible through the NCBI Gene Expression Omnibus accession number GSE101749.

Quantitative real-time RT-PCR

To confirm the transcriptional profiling results, quantitative real-time RT-PCR was performed using the same RNA preparations that were used in the transcriptional profiling experiments. DNase treatment of RNA samples, design of gene-specific primers, and quantitative real-time PCR were performed as described previously (60). The primer sequences for each gene selected for the assays are listed in supplemental Table S7. Data were normalized to an internal control (18S rRNA) and the $\Delta\Delta C_T$ method was used to obtain the relative expression level for each gene.

Genome-wide fitness profiling analysis

This analysis was carried out essentially as previously described (22, 23). Briefly, a pool of haploid-convertible heterozygote diploid yeast deletion mutants was sporulated. Pools of isogenic *MAT*a haploid cells were derived by growth for 2 days on a haploid selection medium (SC-Leu-His-Arg + G418 + canavanine) that either contained or lacked E9591 or LMT. Compound concentrations were 2 μM for E9591 and 1 μM for LMT, resulting in partial growth inhibition of the *ho*Δ mutant, which served as a surrogate wild-type control. Relative representation of each deletion mutant in drug-treated and untreated pools was compared by TAG-array analysis (22, 23). For validation, individual haploid convertible heterozygous diploid mutants were sporulated, spotted onto haploid selec-

tion media with E9591 or LMT at subinhibitory concentrations, and incubated at 30 °C for 3 days.

Mitochondria isolation

An overnight culture of strain S288C was grown in lactate medium as described by Amutha *et al.* (59) and used to inoculate fresh lactate medium (100 ml) at A_{600} of 0.1. After one doubling, E9591, LMT, or DMSO (0.25% v/v) were added to the cultures, and the cells were allowed to grow for 15 h (~4.5 doublings) after treatment. Appropriate compound concentrations, as determined in pilot experiments, were used for the ICP-MS analysis and enzyme assay experiments. The cells were harvested by centrifugation, washed with sterile distilled water, and flash frozen in liquid nitrogen. Mitochondria were isolated using the Yeast Mitochondria Isolation Kit (Sigma). The protein concentration of each fraction was determined using the Pierce BCA Protein Assay Kit (Thermo Fisher Scientific, Waltham, MA). The quality of each mitochondrial fraction was determined by measuring the cytochrome *c* oxidase activity using the Cytochrome *c* Oxidase Assay Kit (Sigma).

Determination of iron concentration by ICP-MS

For determining total iron concentration in whole cells, an overnight culture of strain S288C was grown in SD broth (MOPS buffered, pH 7.0) and used to inoculate fresh medium at A_{600} of 0.1. After one doubling, E9591, LMT, at their respective IC_{50} concentrations, or DMSO (0.25% v/v) was added, and cells were allowed to grow for 15 h (~4.5 doublings). The cells were harvested by centrifugation, washed 3 times with 1 mM EDTA, followed by 3 washes with sterile water, and the pellets were frozen in liquid nitrogen. The cell pellets were treated with 1 ml of 30% (v/v) nitric acid at 120 °C for 20 min in a microwave digester (MARS5, CEM Corp., Matthews, NC). The solution was filtered through a 0.45-μm Teflon filter (Phenomenex, Torrance, CA), and diluted 1:10 with ultrapure water. Dilutions of the multi-element calibration standard 2A (Agilent Technologies, Santa Clara, CA) were prepared in the same concentration of nitric acid as used for the cell extracts. The elemental concentrations of the samples were measured using the Agilent 7500ce ICP-MS system as described previously (65).

For determination of iron in mitochondrial fractions, mitochondria were isolated as described above from S288C cells grown in lactate medium and treated with E9591, LMT, or DMSO for ~4.5 doublings. Mitochondrial fractions containing 250 μg of protein were treated with 0.5 ml of 30% (v/v) nitric acid at 120 °C for 20 min in a microwave digester. The solution was filtered through a 0.45-μm Teflon filter and diluted 1:8 with ultrapure water. Preparation of standards and ICP-MS operating parameters were identical to those described above.

Enzyme assays

For determination of enzyme activity in mitochondrial fractions, mitochondria were isolated as described above from S288C cells grown in lactate medium and treated with E9591, LMT, or DMSO for ~4.5 doublings. Aconitase activity was assayed using the Bioxytech Aconitase-340 Assay Kit (Percipio Biosciences, Manhattan Beach, CA), with two minor modifications. First, mitochondrial fractions were lysed in a homogenization buffer consisting of 0.5% (v/v) Triton X-100 and 50 mM Tris, pH 7.4, prior to addition in the assay (53). Second, 0.6 mM $MnCl_2$ was included in the assay to limit the inactivation of aconitase by superoxide anions (66). Succinate dehydrogenase and malate dehydrogenase activities were measured using colorimetric assay kits (MAK197 and MAK196, respectively) from Sigma.

For assaying the cytosolic Fe-S protein isopropylmalate isomerase (Leu1), the W303-1A yeast strain was used due to high Leu1 activity in this genetic background (32). An overnight culture of strain W303-1A was grown in Synthetic Complete medium (2% (w/v) dextrose, 0.7% (w/v) yeast nitrogen base without amino acids, and 0.1% (w/v) complete supplement mixture, MOPS buffered, and adjusted to pH 7.0) and used to inoculate fresh medium at A_{600} of 0.1. After one doubling, E9591, LMT, at their respective IC_{50} concentrations, or DMSO (0.25%, v/v) was added, and cells were allowed to grow for 15 h (~4.5 doublings) after treatment. Cell harvesting, lysate preparation, and Leu1 enzyme assays were conducted as described previously (67). The same lysates were also used to measure alcohol dehydrogenase activity using a kit (MAK053) from Sigma.

Petite mutant induction assays

The petite-mutant induction assay is based on the principle that yeast cells growing on YPG (glycerol-containing) medium are dependent upon mitochondrial respiration, whereas those growing on YPD (glucose-containing) are not (reviewed in Ref. 41). To determine the rate of formation of petite mutants, an overnight culture of strain S288C was grown in YPD broth and used to inoculate fresh medium at A_{600} of 0.1. After one doubling, E9591 or LMT at their respective IC_{50} concentrations, or DMSO (0.25% v/v) was added, and the cells were allowed to grow for 15 h (~4.5 doublings). Samples from each culture were diluted in YPD broth to obtain 2.5×10^3 cells/ml and plated onto YPD (2% v/v dextrose) and YPG (3% v/v glycerol) plates, and allowed to grow at 30 °C until colonies were formed (3 to 6 days). Colonies were counted, and the percentage of respiration-competent cells was calculated as follows: number of colonies on YPG/number of colonies on YPD $\times$ 100.

Detection of carbonylated proteins

The OxyBlot™ Protein Oxidation Detection Kit from Millipore (Billerica, MA) was used to detect carbonylated proteins. The kit successfully detected carbonylated proteins in a trial experiment on yeast cells exposed to 1 mM H_2O_2 (data not shown). To detect oxidative stress due to E9591 or LMT, an overnight culture of *S. cerevisiae* strain S288C was grown in SD broth (MOPS buffered, pH 7.0) and used to inoculate fresh medium at A_{600} of 0.1. After one doubling, E9591 or LMT at their respective IC_{50} or IC_{75} concentrations, and DMSO was added to the cultures. The cells were allowed to grow for 15 h (~4.5 doublings) after treatment. Protein extract preparation, protein derivatization, and Western analysis were performed as described previously (68).

Drug sensitivity assays

To determine the sensitivities of mutant strains to E9591 and LMT, agar-based drop test assays were performed. Overnight cultures of the mutants and the parent strain BY4743 were grown in YPD-7 (YPD medium, MOPS buffered, pH 7.0) broth (plus 200 μg/ml of G418 in the mutant cultures for selection). The cultures were diluted to an A_{600} of 3.0 and serial dilutions (1:5) were prepared in YPD-7 broth. The dilutions were spotted in 3-μl amounts on YPD-7 agar plates containing 1% (v/v) DMSO, 4 μM E9591, or 5 μM LMT. At these concentrations, the two compounds caused partial growth inhibition of the parent strain. The plates were incubated for 2–3 days at 30 °C.

Author contributions—A. K. A. conceived and coordinated the study and wrote the paper. S. K. T. conducted transcript profiling studies on LMT, and conducted all the experiments shown in Figs. 5–9. T. X. conducted the 4-h transcript profiling studies on E9591, PHEN, and BIPR. Q. F. provided technical assistance in the transcript profiling studies. B. A. and I. A. K. designed and conducted the ICP-MS analysis. X. S. and X. P. designed and conducted the genome-wide fitness profile study. M. M. M. and S. R. B. designed and conducted the quantitative real-time RT-PCR experiments. M. R. J. and S. I. K. conducted the studies shown in Table 1. R. R. and X. C. L. synthesized LMT. A. M. C. provided intellectual input in data interpretation.

References

1. Stévigny, C., Bailly, C., and Quetin-Leclercq, J. (2005) Cytotoxic and antitumor potentialities of aporphinoid alkaloids. *Curr. Med. Chem. Anticancer Agents* **5,** 173–182
2. Guinaudeau, H. (1994) Aporphinoid alkaloids: V. *J. Nat. Prod.* **57,** 1033–1133
3. Hufford, C. D., Liu, S., Clark, A. M., and Oguntimein, B. O. (1987) Anticandidal activity of eupolauridine and onychine, alkaloids from *Cleistopholis patens*. *J. Nat. Prod.* **50,** 961–964
4. Khan, S. I., Nimrod, A. C., Mehrpooya, M., Nitiss, J. L., Walker, L. A., and Clark, A. M. (2002) Antifungal activity of eupolauridine and its action on DNA topoisomerases. *Antimicrob. Agents Chemother.* **46,** 1785–1792
5. Liu, S. C., Oguntimein, B., Hufford, C. D., and Clark, A. M. (1990) 3-Methoxysampangine, a novel antifungal copyrine alkaloid from *Cleistopholis patens*. *Antimicrob. Agents Chemother.* **34,** 529–533
6. Pan, E., Cao, S., Brodie, P. J., Callmander, M. W., Randrianaivo, R., Rakotonandrasana, S., Rakotobe, E., Rasamison, V. E., TenDyke, K., Shen, Y., Suh, E. M., and Kingston, D. G. (2011) Isolation and synthesis of antiproliferative eupolauridine alkaloids of *Ambavia gerrardii* from the Madagascar Dry Forest. *J. Nat. Prod.* **74,** 1169–1174
7. Clark, A. M., Watson, E. S., Ashfaq, M. K., and Hufford, C. D. (1987) *In vivo* efficacy of antifungal oxoaporphine alkaloids in experimental disseminated candidiasis. *Pharm. Res.* **4,** 495–498
8. Hufford, C. D., Funderburk, M. J., Morgan, J. M., and Robertson, L. W. (1975) Two antimicrobial alkaloids from heartwood of *Liriodendron tulipifera* L. *J. Pharm. Sci.* **64,** 789–792
9. Hufford, C. D., Sharma, A. S., and Oguntimein, B. O. (1980) Antibacterial and antifungal activity of liriodenine and related oxoaporphine alkaloids. *J. Pharm. Sci.* **69,** 1180–1183
10. Zhang, Z., ElSohly, H. N., Jacob, M. R., Pasco, D. S., Walker, L. A., and Clark, A. M. (2002) New sesquiterpenoids from the root of *Guatteria multivenia*. *J. Nat. Prod.* **65,** 856–859
11. Chen, C. Y., Wu, H. M., Chao, W. Y., and Lee, C. H. (2013) Review on pharmacological activities of liriodenine. *Afr. J. Pharm. Pharmacol.* **7,** 1067–1070
12. Clark, A. M., and Hufford, C. D. (1992) Antifungal alkaloids. in *The Alkaloids* (Cordell, G. A., ed) pp. 117–150, Academic Press, Inc., San Diego
13. Taghavi-Moghadam, S., Kwong, C. D., Secrist JA 3rd, Khan, S. I., and Clark, A. M. (2016) The synthesis and biological evaluation of alkyl and benzyl naphthyridinium analogs of eupolauridine as potential antimicrobial and cytotoxic agents. *Bioorg. Med. Chem.* **24,** 6119–6130
14. Cyert, M. S., and Philpott, C. C. (2013) Regulation of cation balance in *Saccharomyces cerevisiae*. *Genetics* **193,** 677–713
15. Philpott, C. C., and Protchenko, O. (2008) Response to iron deprivation in *Saccharomyces cerevisiae*. *Eukaryot. Cell* **7,** 20–27
16. Shakoury-Elizeh, M., Tiedeman, J., Rashford, J., Ferea, T., Demeter, J., Garcia, E., Rolfes, R., Brown, P. O., Botstein, D., and Philpott, C. C. (2004) Transcriptional remodeling in response to iron deprivation in *Saccharomyces cerevisiae*. *Mol. Biol. Cell* **15,** 1233–1243
17. Yamaguchi-Iwai, Y., Dancis, A., and Klausner, R. D. (1995) AFT1: a mediator of iron regulated transcriptional control in *Saccharomyces cerevisiae*. *EMBO J.* **14,** 1231–1239
18. Yamaguchi-Iwai, Y., Stearman, R., Dancis, A., and Klausner, R. D. (1996) Iron-regulated DNA binding by the AFT1 protein controls the iron regulon in yeast. *EMBO J.* **15,** 3377–3384
19. Jo, W. J., Kim, J. H., Oh, E., Jaramillo, D., Holman, P., Loguinov, A. V., Arkin, A. P., Nislow, C., Giaever, G., and Vulpe, C. D. (2009) Novel insights into iron metabolism by integrating deletome and transcriptome analysis in an iron deficiency model of the yeast *Saccharomyces cerevisiae*. *BMC Genomics* **10,** 130
20. Puig, S., Askeland, E., and Thiele, D. J. (2005) Coordinated remodeling of cellular metabolism during iron deficiency through targeted mRNA degradation. *Cell* **120,** 99–110
21. Kaplan, J., McVey Ward, D., Crisp, R. J., and Philpott, C. C. (2006) Iron-dependent metabolic remodeling in *S. cerevisiae*. *Biochim. Biophys. Acta* **1763,** 646–651
22. Pan, X., Yuan, D. S., Ooi, S. L., Wang, X., Sookhai-Mahadeo, S., Meluh, P., and Boeke, J. D. (2007) dSLAM analysis of genome-wide genetic interactions in *Saccharomyces cerevisiae*. *Methods* **41,** 206–221
23. Pan, X., Yuan, D. S., Xiang, D., Wang, X., Sookhai-Mahadeo, S., Bader, J. S., Hieter, P., Spencer, F., and Boeke, J. D. (2004) A robust toolkit for functional profiling of the yeast genome. *Mol. Cell* **16,** 487–496
24. Davis-Kaplan, S. R., Ward, D. M., Shiflett, S. L., and Kaplan, J. (2004) Genome-wide analysis of iron-dependent growth reveals a novel yeast gene required for vacuolar acidification. *J. Biol. Chem.* **279,** 4322–4329
25. Lill, R. (2009) Function and biogenesis of iron-sulphur proteins. *Nature* **460,** 831–838
26. Lill, R., Hoffmann, B., Molik, S., Pierik, A. J., Rietzschel, N., Stehling, O., Uzarska, M. A., Webert, H., Wilbrecht, C., and Mühlenhoff, U. (2012) The role of mitochondria in cellular iron-sulfur protein biogenesis and iron metabolism. *Biochim. Biophys. Acta* **1823,** 1491–1508
27. Lill, R., and Mühlenhoff, U. (2006) Iron-sulfur protein biogenesis in eukaryotes: components and mechanisms. *Annu. Rev. Cell Dev. Biol.* **22,** 457–486
28. Lill, R., and Mühlenhoff, U. (2008) Maturation of iron-sulfur proteins in eukaryotes: mechanisms, connected processes, and diseases. *Annu. Rev. Biochem.* **77,** 669–700
29. Babcock, M., de Silva, D., Oaks, R., Davis-Kaplan, S., Jiralerspong, S., Montermini, L., Pandolfo, M., and Kaplan, J. (1997) Regulation of mitochondrial iron accumulation by Yfh1p, a putative homolog of frataxin. *Science* **276,** 1709–1712
30. Garland, S. A., Hoff, K., Vickery, L. E., and Culotta, V. C. (1999) Saccharomyces cerevisiae ISU1 and ISU2: members of a well-conserved gene family for iron-sulfur cluster assembly. *J. Mol. Biol.* **294,** 897–907
31. Jensen, L. T., and Culotta, V. C. (2000) Role of *Saccharomyces cerevisiae* ISA1 and ISA2 in iron homeostasis. *Mol. Cell Biol.* **20,** 3918–3927
32. Kispal, G., Csere, P., Prohl, C., and Lill, R. (1999) The mitochondrial proteins Atm1p and Nfs1p are essential for biogenesis of cytosolic Fe/S proteins. *EMBO J.* **18,** 3981–3989
33. Lange, H., Kaut, A., Kispal, G., and Lill, R. (2000) A mitochondrial ferredoxin is essential for biogenesis of cellular iron-sulfur proteins. *Proc. Natl. Acad. Sci. U.S.A.* **97,** 1050–1055
34. Li, J., Kogan, M., Knight, S. A., Pain, D., and Dancis, A. (1999) Yeast mitochondrial protein, Nfs1p, coordinately regulates iron-sulfur cluster pro-

teins, cellular iron uptake, and iron distribution. *J. Biol. Chem.* **274,** 33025–33034
35. Ramazzotti, A., Vanmansart, V., and Foury, F. (2004) Mitochondrial functional interactions between frataxin and Isu1p, the iron-sulfur cluster scaffold protein, in *Saccharomyces cerevisiae*. *FEBS Lett.* **557,** 215–220
36. Rodríguez-Manzaneque, M. T., Tamarit, J., Bellí, G., Ros, J., and Herrero, E. (2002) Grx5 is a mitochondrial glutaredoxin required for the activity of iron/sulfur enzymes. *Mol. Biol. Cell* **13,** 1109–1121
37. Schilke, B., Voisine, C., Beinert, H., and Craig, E. (1999) Evidence for a conserved system for iron metabolism in the mitochondria of *Saccharomyces cerevisiae*. *Proc. Natl. Acad. Sci. U.S.A.* **96,** 10206–10211
38. Moreno-Cermeño, A., Obis, E., Bellí, G., Cabiscol, E., Ros, J., and Tamarit, J. (2010) Frataxin depletion in yeast triggers up-regulation of iron transport systems before affecting iron-sulfur enzyme activities. *J. Biol. Chem.* **285,** 41653–41664
39. Uzarska, M. A., Dutkiewicz, R., Freibert, S. A., Lill, R., and Mühlenhoff, U. (2013) The mitochondrial Hsp70 chaperone Ssq1 facilitates Fe/S cluster transfer from Isu1 to Grx5 by complex formation. *Mol. Biol. Cell* **24,** 1830–1841
40. Wiedemann, N., Urzica, E., Guiard, B., Müller, H., Lohaus, C., Meyer, H. E., Ryan, M. T., Meisinger, C., Mühlenhoff, U., Lill, R., and Pfanner, N. (2006) Essential role of Isd11 in mitochondrial iron-sulfur cluster synthesis on Isu scaffold proteins. *EMBO J.* **25,** 184–195
41. Contamine, V., and Picard, M. (2000) Maintenance and integrity of the mitochondrial genome: a plethora of nuclear genes in the budding yeast. *Microbiol. Mol. Biol. Rev.* **64,** 281–315
42. Baetz, K., McHardy, L., Gable, K., Tarling, T., Rebérioux, D., Bryan, J., Andersen, R. J., Dunn, T., Hieter, P., and Roberge, M. (2004) Yeast genome-wide drug-induced haploinsufficiency screen to determine drug mode of action. *Proc. Natl. Acad. Sci. U.S.A.* **101,** 4525–4530
43. Deutschbauer, A. M., Jaramillo, D. F., Proctor, M., Kumm, J., Hillenmeyer, M. E., Davis, R. W., Nislow, C., and Giaever, G. (2005) Mechanisms of haploinsufficiency revealed by genome-wide profiling in yeast. *Genetics* **169,** 1915–1925
44. Norris, M., Lovell, S., and Delneri, D. (2013) Characterization and prediction of haploinsufficiency using systems-level gene properties in yeast. *G3 (Bethesda)* **3,** 1965–1977
45. Krogan, N. J., Cagney, G., Yu, H., Zhong, G., Guo, X., Ignatchenko, A., Li, J., Pu, S., Datta, N., Tikuisis, A. P., Punna, T., Peregrín-Alvarez, J. M., Shales, M., Zhang, X., Davey, M., *et al*. (2006) Global landscape of protein complexes in the yeast *Saccharomyces cerevisiae*. *Nature* **440,** 637–643
46. Hausmann, A., Samans, B., Lill, R., and Mühlenhoff, U. (2008) Cellular and mitochondrial remodeling upon defects in iron-sulfur protein biogenesis. *J. Biol. Chem.* **283,** 8318–8330
47. Bellí, G., Molina, M. M., García-Martínez, J., Pérez-Ortín, J. E., and Herrero, E. (2004) *Saccharomyces cerevisiae* glutaredoxin 5-deficient cells subjected to continuous oxidizing conditions are affected in the expression of specific sets of genes. *J. Biol. Chem.* **279,** 12386–12395
48. Sanvisens, N., Bañó, M. C., Huang, M., and Puig, S. (2011) Regulation of ribonucleotide reductase in response to iron deficiency. *Mol. Cell* **44,** 759–769
49. Denning, D. W., and Hope, W. W. (2010) Therapy for fungal diseases: opportunities and priorities. *Trends Microbiol.* **18,** 195–204
50. Dutkiewicz, R., Schilke, B., Cheng, S., Knieszner, H., Craig, E. A., and Marszalek, J. (2004) Sequence-specific interaction between mitochondrial Fe-S scaffold protein Isu and Hsp70 Ssq1 is essential for their *in vivo* function. *J. Biol. Chem.* **279,** 29167–29174
51. Stehling, O., Wilbrecht, C., and Lill, R. (2014) Mitochondrial iron-sulfur protein biogenesis and human disease. *Biochimie* **100,** 61–77
52. Epstein, C. B., Waddle, J. A., Hale, W., 4th, Davé, V., Thornton, J., Macatee, T. L., Garner, H. R., and Butow, R. A. (2001) Genome-wide responses to mitochondrial dysfunction. *Mol. Biol. Cell* **12,** 297–308
53. Chen, O. S., Hemenway, S., and Kaplan, J. (2002) Inhibition of Fe-S cluster biosynthesis decreases mitochondrial iron export: evidence that Yfh1p affects Fe-S cluster synthesis. *Proc. Natl. Acad. Sci. U.S.A.* **99,** 12321–12326
54. Lyons, T. J., Gasch, A. P., Gaither, L. A., Botstein, D., Brown, P. O., and Eide, D. J. (2000) Genome-wide characterization of the Zap1p zinc-responsive regulon in yeast. *Proc. Natl. Acad. Sci. U.S.A.* **97,** 7957–7962
55. Yuan, D. S. (2000) Zinc-regulated genes in *Saccharomyces cerevisiae* revealed by transposon tagging. *Genetics* **156,** 45–58
56. Eide, D. J. (2009) Homeostatic and adaptive responses to zinc deficiency in *Saccharomyces cerevisiae*. *J. Biol. Chem.* **284,** 18565–18569
57. Pagani, M. A., Casamayor, A., Serrano, R., Atrian, S., and Ariño, J. (2007) Disruption of iron homeostasis in *Saccharomyces cerevisiae* by high zinc levels: a genome-wide study. *Mol. Microbiol.* **65,** 521–537
58. Santos, R., Dancis, A., Eide, D., Camadro, J. M., and Lesuisse, E. (2003) Zinc suppresses the iron-accumulation phenotype of *Saccharomyces cerevisiae* lacking the yeast frataxin homologue (Yfh1). *Biochem. J.* **375,** 247–254
59. Amutha, B., Gordon, D. M., Dancis, A., and Pain, D. (2009) Nucleotide-dependent iron-sulfur cluster biogenesis of endogenous and imported apoproteins in isolated intact mitochondria. *Methods Enzymol.* **456,** 247–266
60. Agarwal, A. K., Rogers, P. D., Baerson, S. R., Jacob, M. R., Barker, K. S., Cleary, J. D., Walker, L. A., Nagle, D. G., and Clark, A. M. (2003) Genome-wide expression profiling of the response to polyene, pyrimidine, azole, and echinocandin antifungal agents in *Saccharomyces cerevisiae*. *J. Biol. Chem.* **278,** 34998–35015
61. Simon, R., Lam, A., Li, M. C., Ngan, M., Menenzes, S., and Zhao, Y. (2007) Analysis of gene expression data using BRB-array tools. *Cancer Inform.* **3,** 11–17
62. de Hoon, M. J., Imoto, S., Nolan, J., and Miyano, S. (2004) Open source clustering software. *Bioinformatics* **20,** 1453–1454
63. Saldanha, A. J. (2004) Java Treeview: extensible visualization of microarray data. *Bioinformatics* **20,** 3246–3248
64. Maere, S., Heymans, K., and Kuiper, M. (2005) BiNGO: a Cytoscape plugin to assess overrepresentation of gene ontology categories in biological networks. *Bioinformatics* **21,** 3448–3449
65. Xu, T., Feng, Q., Jacob, M. R., Avula, B., Mask, M. M., Baerson, S. R., Tripathi, S. K., Mohammed, R., Hamann, M. T., Khan, I. A., Walker, L. A., Clark, A. M., and Agarwal, A. K. (2011) The marine sponge-derived polyketide endoperoxide plakortide F acid mediates its antifungal activity by interfering with calcium homeostasis. *Antimicrob. Agents Chemother.* **55,** 1611–1621
66. Lu, C., and Cortopassi, G. (2007) Frataxin knockdown causes loss of cytoplasmic iron-sulfur cluster functions, redox alterations and induction of heme transcripts. *Arch. Biochem. Biophys.* **457,** 111–122
67. Pierik, A. J., Netz, D. J., and Lill, R. (2009) Analysis of iron-sulfur protein maturation in eukaryotes. *Nat. Protoc.* **4,** 753–766
68. Agarwal, A. K., Xu, T., Jacob, M. R., Feng, Q., Lorenz, M. C., Walker, L. A., and Clark, A. M. (2008) Role of heme in the antifungal activity of the azaoxoaporphine alkaloid sampangine. *Eukaryot. Cell* **7,** 387–400